In Vitro Cell.Dev.Biol.—Animal (2012) 48:123–130
DOI 10.1007/s11626-011-9479-3

Impact of medium volume and oxygen concentration in the incubator on pericellular oxygen concentration and differentiation of murine chondrogenic cell culture

Hiroki Oze · Makoto Hirao · Kosuke Ebina · Kenrin Shi · Yoshitaka Kawato · Shoichi Kaneshiro · Hideki Yoshikawa · Jun Hashimoto

Received: 5 October 2011 / Accepted: 22 December 2011 / Published online: 19 January 2012 / Editor: T. Okamoto

Abstract Previous studies have demonstrated that oxygen environment is an important determinate factor of cell phenotypes and differentiation, although factors which affect pericellular oxygen concentration (POC) in murine chondrogenic cell culture remain unidentified. Oxygen concentrations in vivo were measured in rabbit musculoskeletal tissues, which were by far hypoxic compared to 20% O_2 (ranging from 2.29±1.16 to 4.36±0.51%). Oxygen concentrations in murine chondrogenic cell (C3H10T1/2) culture medium were monitored in different oxygen concentrations (20% or 5%) in the incubator and in different medium volumes (3,700 or 7,400 μl) within 25-cm^2 flasks. Chondrogenic differentiation was assessed by glycosaminoglycan production with quantitative evaluation of Alcian blue staining in 12-well culture dishes. Expression of chondrogenic genes, aggrecan, and type II collagen α1, was examined by quantitative real-time polymerase chain reaction. Oxygen concentrations in medium decreased accordingly with the depth from medium surface, and POC at Day 6 was 18.99± 0.81% in 3,700-μl medium (1,480-μm depth) and 13.26± 0.23% in 7,400-μl medium (2,960-μm depth) at 20% O_2 in the incubator, which was 4.96±0.08% (1,480-μm depth) and 2.83±0.42% (2,960-μm depth) at 5% O_2, respectively. The differences of POC compared by medium volume were statistically significant (p=0.0003 at 20% and p=0.001 at 5%). Glycosaminoglycan production and aggrecan gene expression were most promoted when cultured in moderately low POC, 1,000 μl (2,960-μm depth) at 20% O_2 and 500 μl (1,480-μm depth) at 5% O_2 in 12-well culture dishes. We demonstrate that medium volume and oxygen concentration in the incubator affect not only POC but also chondrogenic differentiation.

Keywords Pericellular oxygen concentration · Medium volume · Oxygen concentration · Chondrogenic differentiation

H. Oze · K. Ebina (✉) · K. Shi · Y. Kawato · S. Kaneshiro · H. Yoshikawa
Department of Orthopaedic Surgery,
Osaka University Graduate School of Medicine,
2-2 Yamadaoka,
Suita, Osaka 565-0871, Japan
e-mail: k-ebina@umin.ac.jp

M. Hirao · J. Hashimoto
Department of Rheumatology, Osaka Minami Medical Center,
2-1 Kidohigashi,
Kawachinagano, Osaka 586-8521, Japan

Introduction

It has been recognized that cell proliferation and differentiation, and even phenotypes, are largely influenced by such physical conditions as pH, temperature, gravity, electrical field (Brighton et al. 2008), mechanical factors, and oxygen concentration (Bassett and Herrmann 1961). Among these physical conditions, pericellular oxygen concentration (POC) is thought to be one of the most important factors (Metzen et al. 1995). In cell culture experiments, however, POC is seldom measured but controlled simply by setting the oxygen concentration within the incubator (Wolff et al. 1993; Mamchaoui and Saumon 2000). Pettersen et al. demonstrated that POC in human breast cancer cell culture medium decreased accordingly with the depth from the medium surface and cultured d (Pettersen et al. 2005).

Recent reports have shown that moderate hypoxic condition is suitable not only in most of cell culture but also in most of tissues (Ebbesen et al. 2004; Hopfl et al. 2004). Indeed, it has already been shown that in vivo oxygen concentrations in musculoskeletal tissues are unexpectedly

low; joint cartilage, 1~6% (Kiaer et al. 1988); bone marrow, 1~7% (Richter et al. 1972; Kofoed et al. 1985; Cipolleschi et al. 1993); and muscle, 2~5% (Evers et al. 1997); which are far lower than that of atmosphere as well as general setting of the incubator at 20% O_2. Moreover, we have previously demonstrated that differentiation, transformation, and matrix synthesis of cultured chondrocytic cells are significantly promoted in hypoxic condition with the oxygen concentration setting of the incubator at 5%, although POC in the medium was not measured (Hirao et al. 2006).

However, it still remains unknown whether the difference of oxygen concentration with the incubator and that of medium volume actually affect POC in chondrogenic cell culture. Fortunately, oxygen microsensor and recording system has been developed in recent years, which enabled us to measure oxygen concentration without destroying tissues and cells, in vivo as well as in vitro. In this study, we measured in vivo oxygen concentrations of rabbit musculoskeletal tissues. Then, we assessed whether POC, cell proliferation, and chondrogenic differentiation were influenced by oxygen concentration of the incubator and medium volume in murine pluripotent mesenchymal cell culture, C3H10T1/2 cells, by using this newly developed apparatus.

Materials and Methods

Measurement of oxygen concentrations in vivo. Female New Zealand white rabbits with 3 kg weight were used to measure oxygen concentrations in vivo tissue. Under general anesthesia with intramuscular injection of the mixture of ketamine, xylagine, and midazolam (no respirator or oxygen inhalation was used), oxygen concentrations in knee joints cavity (n=4), articular cartilage surface (n=4), anterior cruciate ligament (n=4), and quadriceps femoris muscles (n=4) were measured by an integrated oxygen microsensor and recording system (PreSens, Regensburg, Germany). Oxygen concentrations (in % or mg/L) were calculated according to protocol of PreSens company. The tip of oxygen microsensor was seated in each compartment of the knee joint and quadriceps femoris muscle as described in Fig. 1.

Cell preparation. C3H10T1/2, murine pluripotent mesenchymal cell line was obtained from RIKEN (RIKEN Bio-Resource Center, Saitama, Japan) and was cultured in Dulbecco's modified Eagle's medium (Invitrogen, Grand Island, NY) supplemented with 10% fetal bovine serum. In all experiments, cells were incubated in 37°C and 5% CO_2.

Measurement of oxygen concentrations in medium and cell proliferation. C3H10T1/2 cells (5×10^4) were seeded in 25-cm^2 tissue culture flasks (Becton Dickinson, Franklin Lakes, NJ) with 2,000-μl medium and incubated in 20% O_2 for the first 24 h. Then, flasks were divided into four groups with different medium volumes (3,700 or 7,400 μl) as well as with different oxygen concentrations (20% or 5%) which were strictly controlled in INVIVO$_2$ 400 Hypoxia Workstation (Ruskinn, Pencoed, UK; Day 0). The depth from medium surface to the bottom of flask was 1,480 μm in 3,700-μl medium and 2,960 μm in 7,400-μl medium, which were equivalent to the depth of 500- and 1,000-μl media, respectively, when applied in 12-well plates. Medium change was done on Day 3. Oxygen concentrations were measured using above described system (PreSens), along vertical transects from 100- to 1,300-μm distance from bottom in

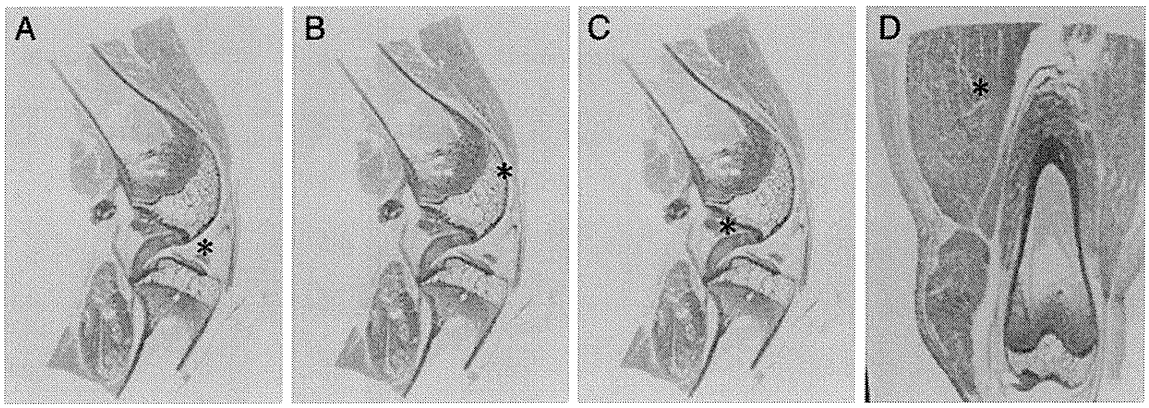

Figure 1. The position of the tip of oxygen microsensor indicated by hematoxylin and eosin staining of rabbit knee joint and quadriceps femoris muscle. Oxygen concentrations were measured in each compartment of the rabbit knee joints and quadriceps femoris muscles with the tip of oxygen microsensor seated at the depth of 10 mm from the anterior surface of patella tendon for knee joint cavity (*A*), at the depth of 5 mm from proximal end of patella for articular cartilage surface (*B*), at the depth of 15 mm from the anterior surface of patella tendon for anterior cruciate ligament (*C*), and at the depth of 15 mm from the anterior surface of the skin and 40 mm proximally from femoral condyle for quadriceps femoris muscles (*D*). The position of the tip of oxygen microsensor is indicated by an *asterisk* (hematoxylin and eosin staining).

Table 1 Oxygen concentrations of rabbit musculoskeletal tissues.

	Knee joint cavity	Cartilage	Anterior cruciate ligament	Muscle
Oxygen concentration (%)	2.92±0.80~3.42±0.85	2.31±2.24~2.48±2.22	3.73±2.33~4.32±2.59	2.29±1.16~4.36±0.51
Oxygen concentration (mg/L)	1.20±0.31~1.41±0.35	1.06±1.03~1.14±1.02	1.71±1.07~1.75±1.19	0.94±0.48~1.76±0.20

Oxygen concentrations of rabbit musculoskeletal tissues were by far hypoxic compared with that of general setting of the incubator (20%). In situ oxygen concentrations of rabbit musculoskeletal tissues. Data are shown as the mean±SD (n=4 knee joint cavity/n=4 articular cartilage surface/n=4 anterior cruciate ligament/n=4 quadriceps femoris muscles)

3,700-μl medium and from 100 to 2,900-μm distance from bottom in 7,400-μl medium. The number of cells was counted on Days 3 and 6 by taking off the cells using 0.25% trypsin EDTA (Invitrogen). All experiments were performed in triplicate.

Cell culture and analysis for chondrogenic differentiation. C3H10T1/2 cells (1×10^5) were seeded in 1,000-μl medium in 12-well plates (Becton Dickinson) and cultured in 20% O_2 for the first 24 h. Then plates were divided into six groups with different medium volumes (500 or 1,000 μl)

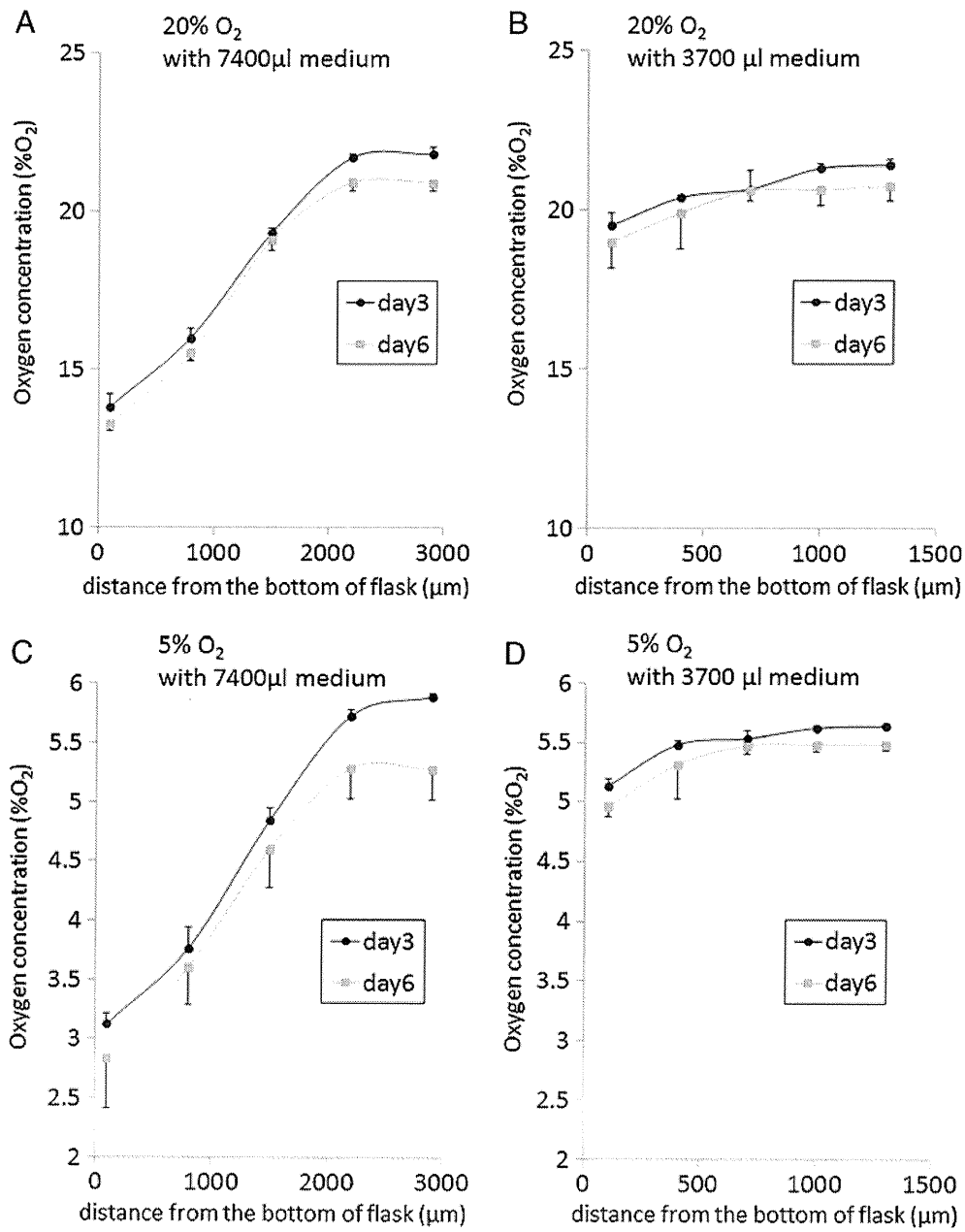

Figure 2. Oxygen concentrations in culture medium decreased accordingly with the distance from the surface and cultured d. Oxygen concentrations in culture medium with the volume of 7,400 μl (*A*, *C*) and 3,700 μl (*B*, *D*) along vertical transects in 25-cm^2 flask were measured on Days 3 and 6, with oxygen concentration set at 20% (*A*, *B*) or 5% (*C*, *D*). The depth from medium surface to the bottom of flask was 2,960 μm in 7,400-μl medium and 1,480 μm in 3,700 μl, which were equivalent to the depth of 1,000 and 500-μl medium in 12-well plate, respectively. Data are shown as mean±SD (n=3).

as well as with different oxygen concentrations (40%, 20%, or 5%) in the incubator, and recombinant human bone morphogenetic protein-2 (BMP-2; Osteopharma, Osaka, Japan) was added to induce chondrogenic differentiation (Day 0). To evaluate chondrogenic matrix synthesis, C3H10T1/2 cells were fixed with 10% formalin, washed with distilled water and 0.1 N HCl, and stained with Alcian blue solution, Alcian blue 8GX (Sigma, St. Louis, MO) on Day 7. For quantitative analysis, the absorbance of Alcian blue dyes bound to sulfated glycosaminoglycan (GAG) was measured at 595 nm, as previously described (Lim et al. 2000). To measure the value of absorbance for Alcian blue relative to cell density, the absorbance data were standardized by total DNA content. Total DNA content was extracted using DNeasy Blood and Tissue Kit (Qiagen, Valencia, CA) and measured. All experiments were performed in triplicate.

Quantitative real-time polymerase chain reaction analysis. Chondrogenic differentiation was evaluated by expression of such genes as *Aggrecan* and typeII collagen α1 (*Col2a1*). Total RNA was extracted from C3H10T1/2 cells with RNeasy Mini Kit (Qiagen), and first-strand cDNA was synthesized using SuperScript III First-Strand Synthesis System (Invitrogen). Then, we proceeded with real-time polymerase chain reaction (PCR) using Light Cycler system (Roche Applied Science, Basel, Switzerland). The SYBR Green assay using Quantitect SYBR Green PCR Kit (Qiagen) was used for all target transcripts. Expression values were standardized by *GAPDH*. The following primers were purchased from Sigma and were used; *Aggrecan* (forward primer 5′-AACTTCTTTGCCACCGGAGA-3′, reverse primer 5′-GGTGCCCTTTTTACACGTGAA-3′); *Col2a1* (forward primer 5′-CCTGTCTGCTTCTTGTAAAAC-3′, reverse primer 5′-AAAAAATACAGAGGTGTTTGACA CAGA-3′); *GAPDH* (forward primer 5′-TGAACGG GAAGCTCACTGG-3′, reverse primer 5′-TCCAC CACCCTGTTGCTGTA-3′). All experiments were performed in triplicate.

Statistical analysis. The results are expressed as the mean± standard deviation. Between-group differences were assessed by Student's *t* test. Values of $p<0.05$ were considered as statistically significant.

Results

Oxygen concentrations in rabbit musculoskeletal tissues. Oxygen concentrations in rabbit musculoskeletal tissues ranged from 2.92±0.80% (1.20±0.31 mg/L) to 3.42± 0.85% (1.41±0.35 mg/L) in knee joint cavity, 2.31±2.24% (1.06±1.03 mg/L) to 2.48±2.22% (1.14±1.02 mg/L) in articular cartilage surface, 3.73±2.33% (1.71±1.07 mg/L) to 4.32±2.59% (1.75±1.19 mg/L) in anterior cruciate ligament, and 2.29±1.16% (0.94±0.48 mg/L) to 4.36±0.51% (1.76±0.20 mg/L) in quadriceps femoris muscles (Table 1). In all tissues, oxygen concentrations were far lower than general oxygen concentration of the incubator, 20%.

Oxygen concentrations in medium and cell proliferation. To assess whether oxygen concentrations within culture medium differ by oxygen concentration in the incubator as well as by the depth from medium surface, we measured oxygen concentrations from the surface to the bottom in 25-cm^2 flasks with different medium volumes (3,700 or 7,400 μl) and with different oxygen concentrations in the incubator (20% or 5%). Oxygen concentrations of medium decreased accordingly with the depth from the surface. POC was 18.99±0.81% in the flask with 3700ul medium (measured at 1,480-μm depth from the surface; equivalent to 500-μl medium in 12-well plate), and 13.26±0.23% in the flask with 7,400-μl medium (measured at 2,960-μm depth from the surface; equivalent to 1,000-μl medium in 12-well plate), respectively, on Day 6 with 20% oxygen concentration in the incubator (Fig. 2*A*, *B*), the two of which showed significant difference ($p=0.0003$).

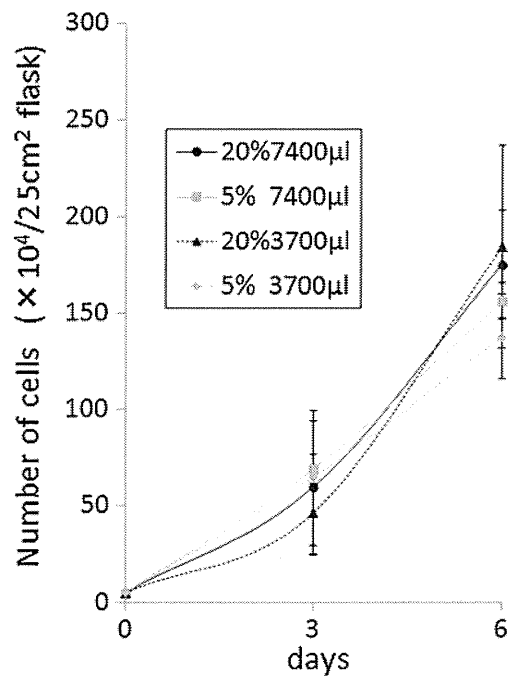

Figure 3. Oxygen concentrations in the incubator and medium volumes had little influence on cell proliferation. The number of C3H10T1/2 cells in culture medium with the volume of 7,400 and 3,700 μl was counted on Days 3 and 6, with oxygen concentration set at 20% or 5% in the incubator. The depth from medium surface to the bottom of flask was 2,960 μm in 7,400-μl medium and 1,480 μm in 3,700 μl, which were equivalent to the depth of 1,000 and 500-μl medium in 12-well plate, respectively. Data are shown as mean±SD ($n=3$).

On the other hand, POC was 4.96±0.08% in the flask with 3,700-μl medium, and 2.83±0.42% in the flask with 7,400-μl medium, respectively, on Day 6 with 5% oxygen concentration in the incubator (Fig. 2*C*, *D*), the two of which also showed significant difference (P=0.001). In spite of the medium change on Day 3, oxygen concentration in the medium on Day 6 showed a tendency to decrease as compared with that on Day 3, but no statistical significance was observed. As shown in Fig. 3, the proliferation of C3H10T1/2 cells showed no significant differences either between different medium volumes or between different oxygen concentrations in the incubator.

Analysis of chondrogenic differentiation. Chondrogenic differentiation of C3H10T1/2 cells was induced by BMP-2 in different medium volumes (500 or 1,000 μl) as well as in different oxygen concentrations in the incubator (40%, 20%, or 5%) in 12-well plates. The depth from medium surface to the bottom of plate was 1,480 μm in 500-μl volume and 2,960 μm in 1,000 μl, respectively. GAG production was most promoted in 1,000 μl with 20% oxygen concentration and in 500 μl with 5% oxygen concentration, the two of which showed no significant difference (Fig. 4*A*, *B*). GAG production in hyper-oxic condition, 40%, was much lower than other

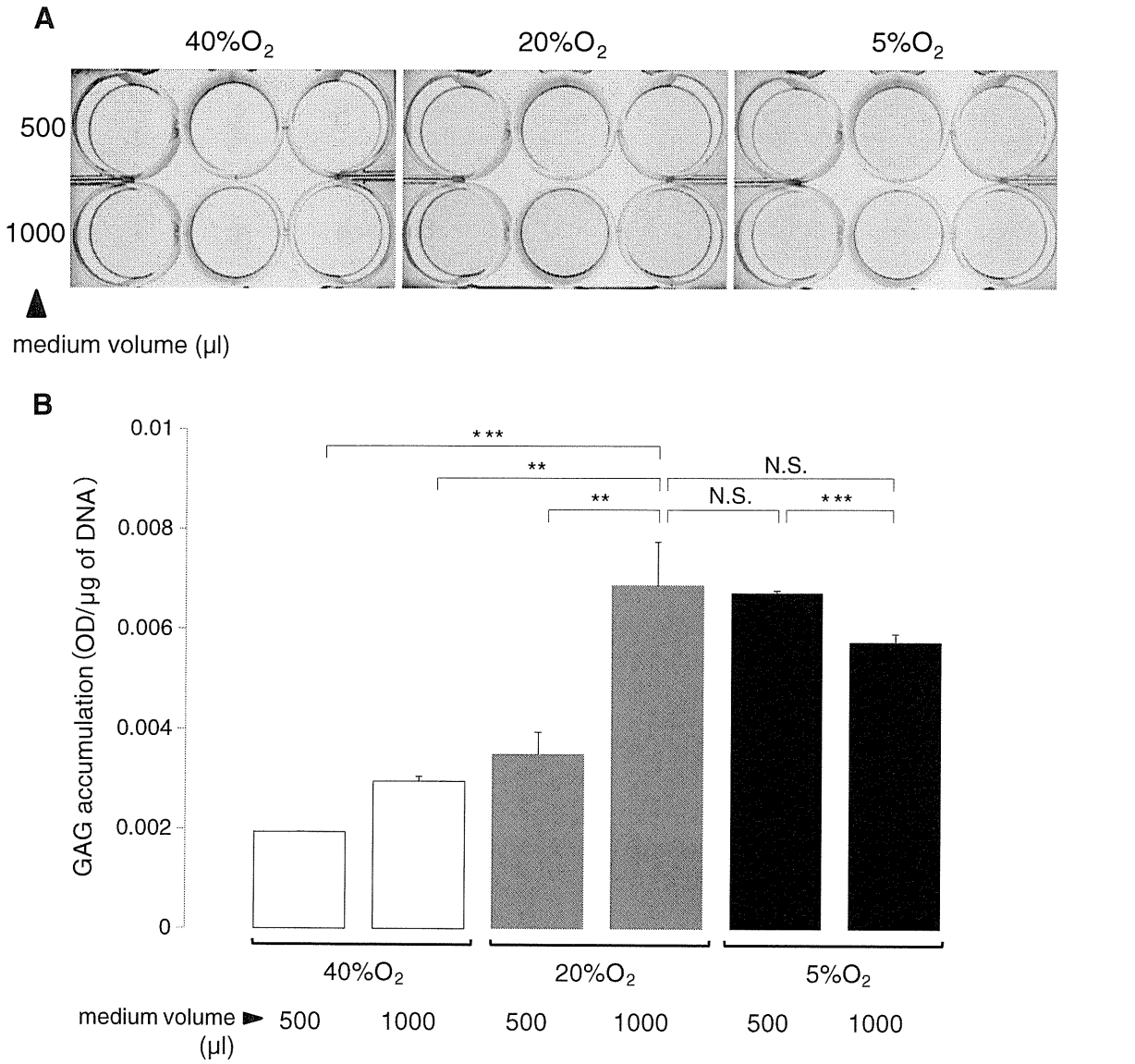

Figure 4. GAG production of C3H10T1/2 cells in 12-well plate culture was most promoted when cultured in 1,000-μl medium at 20% O_2 and in 500-μl medium at 5% O_2 but significantly decreased at 40% O_2. C3H10T1/2 cells were cultured with BMP-2 (300 ng/ml) under 40% or 20% or 5% O_2 in the incubator for 7 d. The cells were stained with Alcian blue (*A*). Quantification of GAG synthesis by C3H10T1/2 cells (*B*). Data are shown as mean±SD (n=3) OD/μg of DNA. *p<0.05; **p<0.01; ***p<0.001; *N.S.* not significant. The depth from medium surface to the bottom of plate was 1,480 μm in 500-μl volume and 2,960 μm in 1,000-μl volume.

oxygen conditions regardless of the medium volume (Fig. 4*A*, *B*). *Aggrecan* mRNA expression was most promoted in 500 μl with 5% oxygen concentration followed by 1,000 μl with 20% oxygen concentration, the two of which still showed no significant difference (Fig. 5*A*). *Aggrecan* mRNA expression in hyper-oxic condition, 40%, was also by far lower than other oxygen conditions regardless of the medium volume (Fig. 5*A*). *Col2a1* mRNA expression was most promoted in 500 μl with 5% oxygen concentration and in both medium volumes at 20% oxygen concentration, which was significantly decreased in 1,000 μl with 5% oxygen concentration and with 40% oxygen concentration (Fig. 5*B*).

Discussion

In this study, we have demonstrated for the first time that the volume of culture medium as well as settings of oxygen concentration in the incubator significantly affected not only

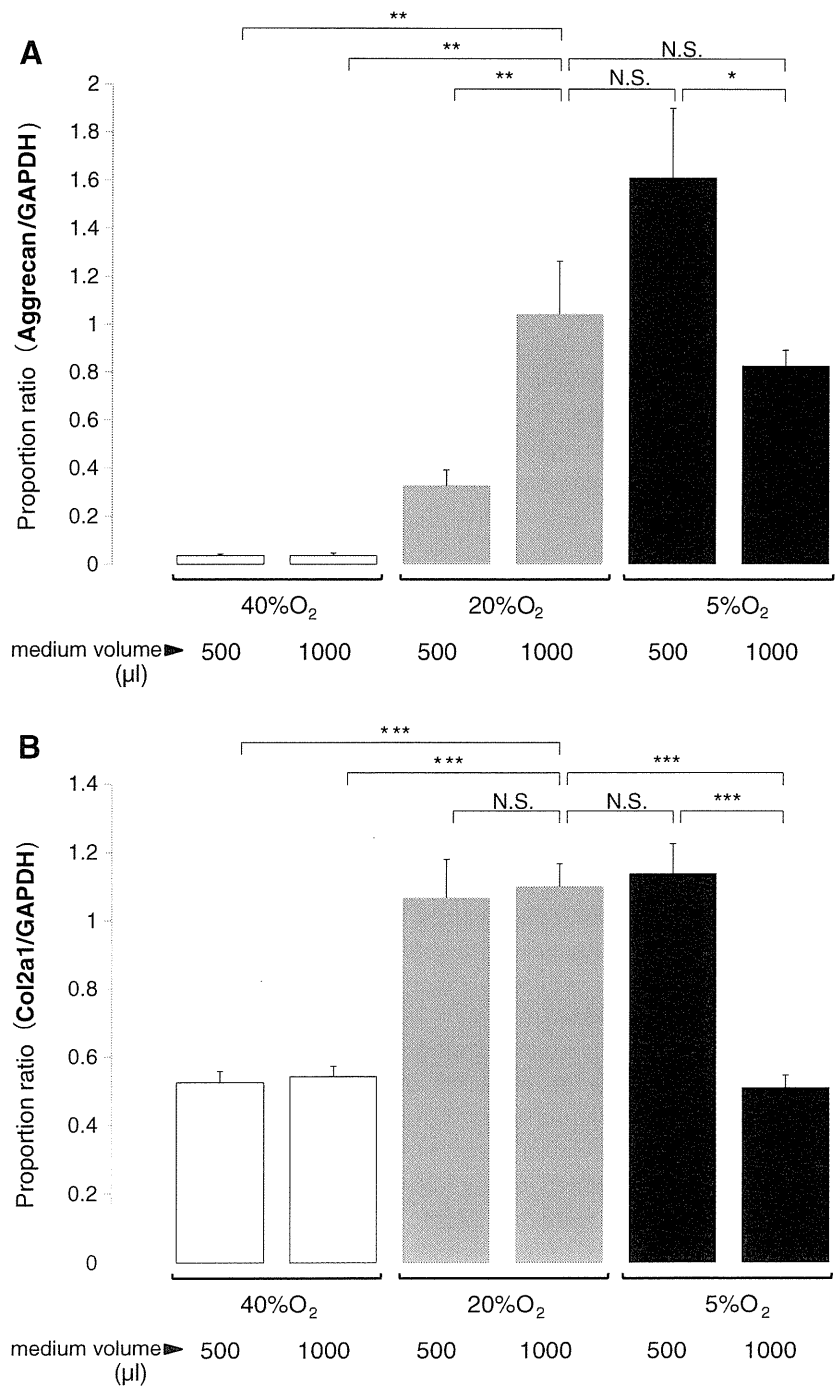

Figure 5. Chondrogenic gene expressions of C3H10T1/2 cells in 12-well plate culture were most promoted in 500 μl medium at 5% O_2 but significantly decreased at 40% O_2. Cells were cultured with BMP-2 (300 ng/ml) under 40% or 20% or 5% O_2 in the incubator. Total RNA was extracted, and the expressions of mRNA for *Aggrecan* (Day 5) (*A*) and *Col2a1* (Day 3) (*B*) were analyzed by real-time PCR. Data are shown as the mean±SD (n=3) of the ratio of *Aggrecan* and *Col2a1* gene expression to *GADPH*. *p<0.05; **p<0.01; ***p<0.001; *N.S.* not significant. The depth from medium surface to the bottom of plate was 1,480 μm in 500-μl volume and 2,960 μm in 1,000-μl volume.

POC but also matrix synthesis and differentiation in murine chondrogenic cell culture. In addition, POC showed a tendency to decrease by cultured days in spite of medium change. This may be the results of increased cell number accompanied by increased cell metabolism (Chapman et al. 1970).

We also measured in vivo oxygen concentrations in rabbit musculoskeletal tissues. The results were compatible with previous reports, supporting the validity of this new, integrated oxygen microsensor and recording system. Moreover, they were about the same as the oxygen concentrations of culture medium with oxygen concentration at 5% in the incubator. From these results, setting at 5%, not at 20% as generally utilized, should be more physiological in chondrogenic cell culture.

As shown in Fig. 3, the proliferation of C3H10T1/2 cells showed no significant differences between oxygen concentrations in the incubator (5% and 20%) as well as between medium volumes (3,700 μl and 7,400 μl), indicating variation of oxygen concentrations in this range have little effect on cell proliferation.

As shown in Figs. 4 and 5, GAG production and *Aggrecan* mRNA expression were most promoted when cultured in 1,000 μl with 20% oxygen concentration (POC, 13.26±0.23%) and in 500 μl with 5% oxygen concentration (POC, 4.96±0.08%), but they significantly decreased in 500 μl with 20% oxygen concentration (POC, 18.99±0.81%). We also cultured the cells in excessive hyper-oxic condition (40% oxygen concentration), and observed that GAG production and expression of both chondrogenic gene, *Aggrecan* and *Col2a1,* were significantly inhibited regardless of medium volume. In addition, Lee et al. demonstrated that chondrogenic differentiation was not significantly affected by the difference of the concentrations (10% and 20%) of fetal bovine serum in the medium (Lee et al. 2006). From these observations, we suppose that the influence of factors accompanied by the change of medium volume such as hydrostatic pressure (Elder et al. 2005; Wagner et al. 2008; Elder and Athanasiou 2009) and growth factors in the medium (Asahina et al. 1996; Shukunami et al. 1998; Haas and Tuan 2000) on chondrogenic differentiation is relatively small, and hyper-oxic condition is simply inappropriate for chondrogenic differentiation.

From our results, hypoxic condition is favorable for chondrogenic differentiation, but at the same time an appropriate oxygen range should exist. GAG production and *Aggrecan* mRNA expression were most promoted with POC ranging from 4.96±0.08 to 13.26±0.23% and were suppressed with that of more than 18.99±0.81%. Moreover, they showed a tendency to decrease in excessive hypoxic condition, 1,000 μl with 5% oxygen concentration (POC, 2.83±0.42%), which is compatible with previous reports stating that severe hypoxia has inhibitory effect on chondrogenic differentiation (Chen et al. 2006; Malladi et al. 2006; Pilgaard et al. 2009). Taken those results together, the appropriate POC range does exist, so medium volume and oxygen concentration in the incubator should be considered in each chondrogenic cell experiment.

There are several limitations in this study. Since we used 25-cm^2 flasks in monitoring oxygen concentration due to unsolvable difficulties in monitoring it in 12-well plates, POC in these two kinds of containers might have been different from each other, though we applied the calculated amount of medium in each container to standardize to the same depth in both.

In this study, *Col2a1* mRNA expression was suppressed with POC less than 4.96±0.08%, while oxygen concentrations in compartments of the rabbit knee joints varied from 2.31±2.24 to 4.32±2.59%. There might be some discrepancies in appropriate oxygen concentrations between in vivo and in vitro. Also, prolonged culture period may induce further hypoxic condition and affect chondrogenic differentiation, but we studied only within 7 d of culture period in this study, which may be another limitation.

From the results of our in vivo and in vitro study, we conclude that moderate hypoxic condition controlled by medium volume and oxygen concentration in the incubator can be a crucial factor in murine chondrogenic cell culture. These findings could be important information not only in in vitro experiments in the field of cell biology but also in donor cell culture in regenerative medicine in the near future.

Acknowledgments We would like to thank Mari Shinkawa for her excellent technical assistances, and we also would like to thank Osteopharma for supplying recombinant human BMP-2.

References

Asahina I.; Sampath T. K.; Hauschka P. V. Human osteogenic protein-1 induces chondroblastic, osteoblastic, and/or adipocytic differentiation of clonal murine target cells. *Exp. Cell Res.* 222: 38–47; 1996.

Bassett C. A.; Herrmann I. Influence of oxygen concentration and mechanical factors on differentiation of connective tissues in vitro. *Nature* 190: 460–461; 1961.

Brighton C. T.; Wang W.; Clark C. C. The effect of electrical fields on gene and protein expression in human osteoarthritic cartilage explants. *J. Bone Joint Surg. Am.* 90: 833–848; 2008.

Chapman J. D.; Sturrock J.; Boag J. W.; Crookall J. O. Factors affecting the oxygen tension around cells growing in plastic Petri dishes. *Int. J. Radiat. Biol. Relat. Stud. Phys. Chem. Med.* 17: 305–328; 1970.

Chen L.; Fink T.; Ebbesen P.; Zachar V. Hypoxic treatment inhibits insulin-induced chondrogenesis of ATDC5 cells despite upregulation of DEC1. *Connect. Tissue Res.* 47: 119–123; 2006.

Cipolleschi M. G.; Dello Sbarba P.; Olivotto M. The role of hypoxia in the maintenance of hematopoietic stem cells. *Blood* 82: 2031–2037; 1993.

Ebbesen P.; Eckardt K. U.; Ciampor F.; Pettersen E. O. Linking measured intercellular oxygen concentration to human cell functions. *Acta Oncol.* 43: 598–600; 2004.

Elder B. D.; Athanasiou K. A. Hydrostatic pressure in articular cartilage tissue engineering: from chondrocytes to tissue regeneration. *Tissue Eng. Part B Rev.* 15: 43–53; 2009.

Elder S. H.; Fulzele K. S.; McCulley W. R. Cyclic hydrostatic compression stimulates chondroinduction of C3H/10T1/2 cells. *Biomech. Model. Mechanobiol.* 3: 141–146; 2005.

Evers B.; Odemis V.; Gerngross H. Oxygen partial pressure in the anterior tibial muscle during and after knee surgery with tourniquet control. *Adv. Exp. Med. Biol.* 428: 317–325; 1997.

Haas A. R.; Tuan R. S. Murine C3H10T1/2 multipotential cells as an in vitro model of mesenchymal chondrogenesis. *Methods Mol. Biol.* 137: 383–389; 2000.

Hirao M.; Tamai N.; Tsumaki N.; Yoshikawa H.; Myoui A. Oxygen tension regulates chondrocyte differentiation and function during endochondral ossification. *J. Biol. Chem.* 281: 31079–31092; 2006.

Hopfl G.; Ogunshola O.; Gassmann M. HIFs and tumors—causes and consequences. *Am. J. Physiol. Regul. Integr. Comp. Physiol.* 286: R608–R623; 2004.

Kiaer T.; Gronlund J.; Sorensen K. H. Subchondral pO_2, pCO_2, pressure, pH, and lactate in human osteoarthritis of the hip. *Clin. Orthop. Relat. Res.* 229: 149–155; 1988.

Kofoed H.; Sjontoft E.; Siemssen S. O.; Olesen H. P. Bone marrow circulation after osteotomy. Blood flow, pO_2, pCO_2, and pressure studied in dogs. *Acta Orthop. Scand.* 56: 400–403; 1985.

Lee C. C.; Ye F.; Tarantal A. F. Comparison of growth and differentiation of fetal and adult rhesus monkey mesenchymal stem cells. *Stem Cells Dev.* 15: 209–220; 2006.

Lim Y. B.; Kang S. S.; Park T. K.; Lee Y. S.; Chun J. S.; Sonn J. K. Disruption of actin cytoskeleton induces chondrogenesis of mesenchymal cells by activating protein kinase C-alpha signaling. *Biochem. Biophys. Res. Commun.* 273: 609–613; 2000.

Malladi P.; Xu Y.; Chiou M.; Giaccia A. J.; Longaker M. T. Effect of reduced oxygen tension on chondrogenesis and osteogenesis in adipose-derived mesenchymal cells. *Am. J. Physiol. Cell Physiol.* 290: C1139–C1146; 2006.

Mamchaoui K.; Saumon G. A method for measuring the oxygen consumption of intact cell monolayers. *Am. J. Physiol. Lung Cell. Mol. Physiol.* 278: L858–L863; 2000.

Metzen E.; Wolff M.; Fandrey J.; Jelkmann W. Pericellular pO_2 and O_2 consumption in monolayer cell cultures. *Respir. Physiol.* 100: 101–106; 1995.

Pettersen E. O.; Larsen L. H.; Ramsing N. B.; Ebbesen P. Pericellular oxygen depletion during ordinary tissue culturing, measured with oxygen microsensors. *Cell Prolif.* 38: 257–267; 2005.

Pilgaard L.; Lund P.; Duroux M.; Fink T.; Ulrich-Vinther M.; Soballe K.; Zachar V. Effect of oxygen concentration, culture format and donor variability on in vitro chondrogenesis of human adipose tissue-derived stem cells. *Regen. Med.* 4: 539–548; 2009.

Richter A.; Sanford K. K.; Evans V. J. Influence of oxygen and culture media on plating efficiency of some mammalian tissue cells. *J. Natl. Cancer Inst.* 49: 1705–1712; 1972.

Shukunami C.; Ohta Y.; Sakuda M.; Hiraki Y. Sequential progression of the differentiation program by bone morphogenetic protein-2 in chondrogenic cell line ATDC5. *Exp. Cell Res.* 241: 1–11; 1998.

Wagner D. R.; Lindsey D. P.; Li K. W.; Tummala P.; Chandran S. E.; Smith R. L.; Longaker M. T.; Carter D. R.; Beaupre G. S. Hydrostatic pressure enhances chondrogenic differentiation of human bone marrow stromal cells in osteochondrogenic medium. *Ann. Biomed. Eng.* 36: 813–820; 2008.

Wolff M.; Fandrey J.; Jelkmann W. Microelectrode measurements of pericellular pO_2 in erythropoietin-producing human hepatoma cell cultures. *Am. J. Physiol.* 265: C1266–C1270; 1993.

Development 139, 1153-1163 (2012) doi:10.1242/dev.072652

SIK3 is essential for chondrocyte hypertrophy during skeletal development in mice

Satoru Sasagawa[1,3,6], Hiroshi Takemori[4], Tatsuya Uebi[4], Daisuke Ikegami[1,2], Kunihiko Hiramatsu[1,2], Shiro Ikegawa[5], Hideki Yoshikawa[2] and Noriyuki Tsumaki[1,2,3,7,*]

SUMMARY

Chondrocyte hypertrophy is crucial for endochondral ossification, but the mechanism underlying this process is not fully understood. We report that salt-inducible kinase 3 (SIK3) deficiency causes severe inhibition of chondrocyte hypertrophy in mice. SIK3-deficient mice showed dwarfism as they aged, whereas body size was unaffected during embryogenesis. Anatomical and histological analyses revealed marked expansion of the growth plate and articular cartilage regions in the limbs, accumulation of chondrocytes in the sternum, ribs and spine, and impaired skull bone formation in SIK3-deficient mice. The primary phenotype in the skeletal tissue of SIK3-deficient mice was in the humerus at E14.5, where chondrocyte hypertrophy was markedly delayed. Chondrocyte hypertrophy was severely blocked until E18.5, and the proliferative chondrocytes occupied the inside of the humerus. Consistent with impaired chondrocyte hypertrophy in SIK3-deficient mice, native SIK3 expression was detected in the cytoplasm of prehypertrophic and hypertrophic chondrocytes in developing bones in embryos and in the growth plates in postnatal mice. HDAC4, a crucial repressor of chondrocyte hypertrophy, remained in the nuclei in SIK3-deficient chondrocytes, but was localized in the cytoplasm in wild-type hypertrophic chondrocytes. Molecular and cellular analyses demonstrated that SIK3 was required for anchoring HDAC4 in the cytoplasm, thereby releasing MEF2C, a crucial facilitator of chondrocyte hypertrophy, from suppression by HDAC4 in nuclei. Chondrocyte-specific overexpression of SIK3 induced closure of growth plates in adulthood, and the SIK3-deficient cartilage phenotype was rescued by transgenic SIK3 expression in the humerus. These results demonstrate an essential role for SIK3 in facilitating chondrocyte hypertrophy during skeletogenesis and growth plate maintenance.

KEY WORDS: *Col11a2*, HDAC4, SIK3, Chondrocyte hypertrophy, Endochondral bone formation, Knockout mouse

INTRODUCTION

Vertebrate bones develop through membranous or endochondral ossification. Except for craniofacial bones and the clavicle, all bones are established through the latter process (Olsen et al., 2000; Karsenty et al., 2009). At the onset of endochondral bone formation, mesenchymal cells first undergo condensation, followed by differentiation of cells within these condensations into chondrocytes. Chondrocytes then proliferate and produce extracellular matrix to form the primordial cartilage that prefigures the future skeletal elements. Shortly after the formation of the primordial cartilage, proliferating chondrocytes in the central region of the cartilage exit the cell cycle and differentiate into prehypertrophic, and subsequently hypertrophic, chondrocytes. The proliferating chondrocytes closest to the prehypertrophic chondrocytes flatten out and form orderly columns of flat chondrocytes that continue to proliferate. Finally, hypertrophic chondrocytes progress to terminal maturation, following which they express matrix metalloproteinase 13 (MMP13). The terminally matured chondrocytes undergo apoptosis. Blood vessels, along with osteoblasts, osteoclasts and hematopoietic cells, then invade this region and form primary ossification centers. Within these centers, the hypertrophic cartilage matrix is degraded, the hypertrophic chondrocytes die, and bone replaces the disappearing cartilage.

Recent molecular and genetic studies coupled with classical histological approaches have revealed many of the factors that are involved in endochondral bone formation (Lefebvre and Smits, 2005). For example, SOX9 is expressed in mesenchymal progenitor cells and in chondrocytes, but its expression ceases in prehypertrophic chondrocytes (Ng et al., 1997; Zhao et al., 1997). SOX9 has a variety of functions in chondrogenesis: its expression in mesenchymal progenitor cells is essential for cartilage formation (Akiyama et al., 2002); it directly regulates cartilage-specific matrix genes such as the α1(II) collagen chain gene (*Col2a1*), aggrecan (*Acan*) and the α2(XI) collagen chain gene (*Col11a2*); it sustains the survival of proliferative chondrocytes during development (Ikegami et al., 2011); SOX9 overexpression in proliferative chondrocytes suppresses their hypertrophy (Akiyama et al., 2004); and it negatively regulates the transcription of the gene that encodes vascular endothelial growth factor (VEGF), which is expressed by hypertrophic chondrocytes (Hattori et al., 2010).

Regarding the hypertrophic differentiation of chondrocytes, several crucial transcriptional regulators have been identified. Histone deacetylase 4 (HDAC4), a class II HDAC, represses the expression of multiple genes through chromatin remodeling, thereby regulating cell fate. To elucidate the specific role of HDAC4, *Hdac4*-null mice have been generated and were noted to display dwarfism and inappropriate chondrocyte hypertrophy,

[1]Department of Bone and Cartilage Biology, Graduate School of Medicine, Osaka University, 2-2 Yamadaoka, Suita, Osaka 565-0871, Japan. [2]Department of Orthopedic Surgery, Graduate School of Medicine, Osaka University, 2-2 Yamadaoka, Suita, Osaka 565-0871, Japan. [3]Japan Science and Technology Agency, CREST, Tokyo, 102-0075, Japan. [4]Laboratory of Cell Signal and Metabolism, National Institute of Biomedical Innovation, 7-6-9 Asagi, Ibaraki, Osaka 567-0085, Japan. [5]Laboratory of Bone and Joint Diseases, Center for Genomic Medicine, RIKEN, Tokyo 108-8639, Japan. [6]Department of Biology, Osaka Medical Center for Cancer and Cardiovascular Diseases, Osaka 537-0025, Japan. [7]Center for iPS Cell Research and Application, Kyoto-University, 53 Kawahara-cho, Shogoin, Sakyo-ku, Kyoto 606-8507, Japan.

*Author for correspondence (ntsumaki@cira.kyoto-u.ac.jp)

Accepted 5 January 2012

leading to ectopic bone formation. By contrast, the overexpression of HDAC4 in proliferative chondrocytes inhibited chondrocyte hypertrophy (Vega et al., 2004).

The transcription factor RUNX2 (CBFA1) is a key regulator of osteoblast differentiation. When RUNX2-deficient mice were generated, a lack of chondrocyte hypertrophy was found, suggesting that RUNX2 might regulate chondrocyte hypertrophy as does HDAC4 (Komori et al., 1997). To address this possibility, non-hypertrophic chondrocyte-specific *Runx2* transgenic mice were generated. These animals showed ectopic chondrocyte hypertrophy and enhanced endochondral ossification (Takeda et al., 2001). MEF2C is a crucial transcription factor in muscle and cardiovascular development. To clarify its role in chondrogenesis, cartilage-specific conditional *Mef2c* deletion mice and cartilage-specific dominant-negative and dominant-active MEF2C mice were generated, and these demonstrated a positive role for MEF2C in chondrocyte hypertrophy (Arnold et al., 2007). Genetically, the mild phenotype in the sternum of $Mef2c^{+/-}$ pups was rescued by deletion of one copy of the *Hdac4* gene, demonstrating that it depends on a balance between transcriptional activation by MEF2C and repression by HDAC4 (Arnold et al., 2007). In addition, HDAC4 interacts directly with RUNX2 to repress its transcriptional activity on the type X collagen promoter (Vega et al., 2004). Therefore, HDAC4 is thought to be a central negative regulator of chondrocyte hypertrophy.

With regard to the regulation of HDAC4 activity in chondrocyte hypertrophy, a recent study proposed that phosphatase PP2A, which is activated by the PTHrP-cAMP-PKA cascade in chondrocytes, dephosphorylates HDAC4 to turn on its activity and to potentiate its localization in nuclei, thereby inhibiting chondrocyte hypertrophy (Kozhemyakina et al., 2009). However, the regulatory mechanisms that suppress the transcriptional repression activity of HDAC4 in chondrocytes have not been reported so far.

Salt-inducible kinase 3 (SIK3, also known as QSK) is a member of the 5′-AMP-activated protein kinase (AMPK) family. SIK3 belongs to the SIK subfamily, which also includes SIK1 (also known as MSK or SNF1LK) and SIK2 (also known as QIK) (Katoh et al., 2004). Mammalian SIK1 and SIK2 are currently being characterized in terms of their function in various biological processes and molecular regulatory mechanisms. Recently, fly SIK3 (the homolog of mouse SIK2) was shown to sequester HDAC4 in the cytoplasm and to regulate the energy balance in the *Drosophila* fat body (Wang et al., 2011). Compared with SIK1 and SIK2, the function of SIK3 is poorly understood. To understand SIK3 function in vertebrates, we generated SIK3-deficient mice. The SIK3-deficient mice showed various phenotypes, including bone abnormalities (this study) and impaired cholesterol metabolism (T.U., Y. Itoh, O. Hatano, A. Kumagai, M. Sanosaka, T. Sasaki, S.S., J. Doi, K. Tatsumi, K. Mitamura et al., unpublished). Here, we report a role for SIK3 in skeletal development. By performing anatomical and histological analyses, we clarified that the bone abnormalities in SIK3-deficient mice are due to impaired chondrocyte hypertrophy. We also demonstrated that SIK3 binds directly to HDAC4 and has the capacity to anchor HDAC4 in the cytoplasm. Together, our results establish SIK3 as an essential factor for chondrocyte hypertrophy.

MATERIALS AND METHODS

Generation of *Sik3* knockout mice and embryos

The *Sik3* knockout strategy and targeting vector design are shown in supplementary material Fig. S1. Briefly, the PGK-neo cassette was inserted in place of exon 1 of *Sik3*. The successful targeting of embryonic stem cells was confirmed by Southern blot analysis, and the cells were injected into C57BL/6N blastocysts. To obtain SIK3-deficient embryos, *Sik3* heterozygous male and female mice were mated and wild-type littermates were used as controls.

Generation of *Col11a2-hSIK3* transgenic mice

The α2(XI) collagen gene-based expression vector 742LacZInt contains the mouse *Col11a2* promoter (–742 to +380), an SV40 RNA splice site, the *lacZ* reporter gene, SV40 polyadenylation signal and a 2.3 kb segment of the first intron of *Col11a2* as an enhancer (Tsumaki et al., 1996). To create the human *SIK3* (*hSIK3*) transgene, the *hSIK3* fragment was cloned into the expression vector, replacing the *lacZ* gene, to create *Col11a2-hSIK3*. Transgenic mice were produced by microinjection of the linearized insert into the pronuclei of fertilized eggs from F1 hybrid mice (C57BL/6 × DBA), as described previously (Hiramatsu et al., 2011). Transgenic mice were identified by PCR assays on genomic DNA extracted from the tail. The mice were backcrossed at least eight times to the C57BL/6N strain.

All experiments were approved by the Institutional Animal Care and Use Committee (IACUC) of Osaka University Graduate School of Medicine and the Osaka University Living Modified Organism (LMO) Experiments Safety Committee.

Cartilage and bone staining

For whole-mount skeletal analysis, mice or embryos were skinned, the internal organs and as much connective tissue as possible, including muscles and tendons, were removed, and the specimens fixed overnight in pure ethanol. The specimens were stained with Alcian Blue and Alizarin Red for 48 hours for embryos or 72 hours for adult mice. After staining, embryos were incubated in 20% glycerol in a 1% KOH solution and adult specimens were incubated in 3% KOH solution at 37°C for 1 day to remove soft tissue. To improve transparency, specimens were cleared in 50% glycerol in a 0.5% KOH solution at 37°C for 2 days, which was then replaced with 80% glycerol solution for completion of the reaction.

Sectioning and staining

For juvenile and adult mouse samples, specimens were fixed in 10% phosphate-buffered formalin at 4°C for 16-24 hours, followed by decalcification with saturated EDTA solution for 4 days. For embryonic samples, specimens were fixed in 4% PFA in PBS at 4°C for 16 hours, followed by decalcification with saturated EDTA solution for 1 day, except for specimens younger than E18.5 and samples used for von Kossa staining. The samples were embedded in paraffin, sectioned at 3 μm, and then subjected to Safranin O and Fast Green staining or von Kossa staining according to standard protocols.

Immunofluorescent and immunohistochemical staining

Antibodies used for the immunofluorescent analysis of section samples were as follows: mouse anti-type I collagen (Abcam, 1:500), mouse anti-type II collagen (Thermo Scientific, 1:500), mouse anti-type X collagen (Quartett, 1:100), goat anti-MMP13 (Millipore, 1:100), rabbit anti-SOX9 (Santa Cruz Biotechnology, 1:100), mouse anti-PCNA (Santa Cruz, 1:100), rabbit anti-SIK3 (Abcam, 1:100), rabbit anti-HDAC4 (Abcam, 1:100), rabbit anti-MEF2C (Abcam, 1:100), Alexa Fluor-conjugated secondary antibodies (Invitrogen, 1:500) and an HRP-labeled secondary antibody (GE Healthcare, 1:500).

Deparaffinized specimens were incubated in 20 mM Tris-HCl (pH 9.0) at 70°C for 6 hours to retrieve the antigen. For detection of type II collagen, samples were treated with 20 μM proteinase K for 10 minutes at 37°C. After blocking with 2% blocking reagent (Roche), the specimens were stained with primary antibody at 4°C overnight, then rinsed twice with PBS, and stained with a secondary antibody for 2 hours, followed by nuclear counterstaining with Hoechst 33342 (Invitrogen, 1:1000) for 30 minutes or, for samples used for detection of type II collagen, with Hematoxylin at room temperature. Specimens were observed using a fluorescence microscope system (Eclipse Ti, Nikon) equipped with a CCD camera (Hamamatsu Photonics). HRP labeling was visualized with DAB reagent (DAKO).

Cell culture, transfection, pulldown assay and imaging

293FT cells were grown in DMEM containing 10% FBS. ATDC5 cells were grown in DMEM/F-12 medium containing 5% FBS. The *Hdac4* and *Mef2c* cDNAs were cloned from a primary chondrocyte cDNA pool into the pENTR vector (Invitrogen) and their sequences confirmed. The primer sequences used for cloning are listed in supplementary material Table S1. Full-length *Sik3* cDNA was purchased from Invitrogen. For HA-tagged HDAC4 expression, *Hdac4* cDNA was subcloned into the pCMV-HA expression vector (Clontech). To construct an EGFP- HDAC4 fusion expression vector, the *Egfp* gene was subcloned into the 5′ region of the *Hdac4* gene in pENTR-Hdac4. For other expression constructs, the cDNAs were transferred into the CMV-driven expression vector using the Gateway system (Invitrogen). For transient transfection, Lipofectamine 2000 (Invitrogen) was used according to the manufacturer's instructions.

The pulldown assay was performed as described previously (Takeda et al., 2006). Briefly, transiently transfected cells were solubilized in RIPA buffer containing protease inhibitor and phosphatase inhibitor (both Roche) 48 hours after transfection. The cell lysates in RIPA buffer were subjected to pulldown assay with the 12CA5 anti-HA or 9E10 anti-Myc antibody (Santa Cruz) and Protein G Sepharose beads (GE Healthcare), were separated on a NuPAGE gel (Invitrogen) and evaluated by a western blotting analysis with the ECL system (PerkinElmer). A ChemiDoc XRS Plus system (BioRad) was used for image development.

For cellular immunofluorescence imaging, cells were fixed in 10% PFA for 30 minutes at room temperature, washed twice with PBS, and then permeabilized with 0.2BT solution (0.2% Triton X-100 and 2 mg/ml BSA in water) for 10 minutes. The specimens were stained with anti-SIK3 antibody (1:500) for 2 hours, followed by an Alexa Fluor-conjugated secondary antibody (1:2000) for 1 hour, and were then counterstained with Hoechst 33342 (1:1000) for 30 minutes at room temperature. The cells were imaged using a fluorescence microscope (Eclipse Ti) equipped with a CCD camera (Hamamatsu Photonics).

MEF2C luciferase reporter assays were performed as described previously (Takemori et al., 2009). The constitutively active form of SIK3 (T163E, S494A) (Katoh et al., 2006) was used in the ATDC5 cells.

Quantitative PCR

Humeri were isolated from E18.5 embryos and tissues were crushed by vigorous shaking with beads. Total RNA was purified using an RNA purification kit (Qiagen). For cDNA synthesis, Superscript III (Invitrogen) was used according to the manufacturer's protocol. The primers used are listed in supplementary material Table S1. The PCR reaction was performed with CYBR premix reagent (TaKaRa) and the 7900HT Fast Real-Time PCR system (Applied Biosystems).

Statistical analysis

Statistically significant differences between groups were evaluated by Student's *t*-test. $P<0.05$ was considered statistically significant. The analyses were performed using Excel (Microsoft) and Statcel3 (OMS Publishing).

RESULTS

SIK3-deficient mice have skeletal defects

Although $Sik3^{-/-}$ mice were born at the expected Mendelian frequency, 90% died on the first day after birth (T.U., Y. Itoh, O. Hatano, A. Kumagai, M. Sanosaka, T. Sasaki, S.S., J. Doi, K. Tatsumi, K. Mitamura et al., unpublished). The surviving SIK3-deficient mice showed dwarfism throughout their postnatal life. The mean weight of $Sik3^{-/-}$ mice was 7 g, whereas that of $Sik3^{+/+}$ and $Sik3^{+/-}$ mice was 13 g at 3 weeks of age. Because an X-ray analysis revealed that they had bone deformities, we focused on the skeletal abnormality as a SIK3-deficient phenotype. Anatomical examination of SIK3-deficient mice revealed numerous skeletal abnormalities (Fig. 1). When each of the skeletal elements of SIK3-deficient mice (4 months old) were compared with those of age-matched wild-type mice, we found that they had a shorter sternum

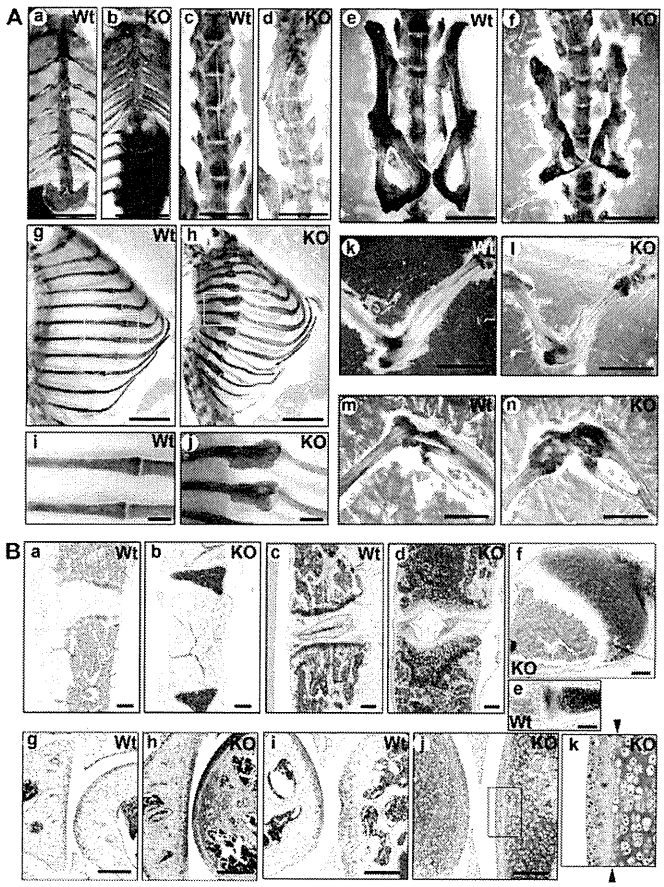

Fig. 1. Skeletal deformity in SIK3-deficient mice. (**A**) Skeletal elements from wild-type (Wt) and SIK3-deficient (KO) mice at 4 months of age stained with Alizarin Red and Alcian Blue: sternum (a,b), spine (c,d, front view), pelvis (e,f), ribcage (g,h, lateral view) and each junction (i,j), elbow (k,l) and knee (m,n). (**B**) Histological sections from wild-type and SIK3-deficient mice at 4 months of age (except for the rib junction, which was examined at 3 months of age) stained with Safranin O, Fast Green and Iron Hematoxylin: sternum (a,b), spine (c,d), rib junction (e,f), elbow (g,h) and knee (i,j), and a higher magnification view of articular cartilage regions of the knee (k). Arrowheads indicate the tide line. Scale bars: 5 mm in Aa-h; 1 mm in Ai,j; 200 μm in B.

with low mineralization (Fig. 1Aa,b), a thinner spine that was twisted as in scoliosis (Fig. 1Ac,d), a hypoplastic pelvis (Fig. 1Ae,f), short mineralized ribs with an abnormal mass at the junction between the bone and cartilage, which was similar in appearance to a rachitic rosary (Fig. 1Ag-j), and shorter long bones (Fig. 1Ak,l) with epiphyseal and metaphysial expansion of the limb joint region (Fig. 1Am,n). In SIK3-deficient mice, delayed membranous ossification of the skull bones was observed on postnatal day (P) 1 (supplementary material Fig. S2A,B). The parietal bone had an immature appearance from the juvenile stage until 8 months of age (supplementary material Fig. S2C-H, asterisks) and the sutures remained loosely closed throughout adulthood (supplementary material Fig. S2C-H, arrowheads). A large fontanelle remained open from juvenile stage until adulthood (supplementary material Fig. S2C-H, arrows), whereas it was already closed in 3-week-old wild-type mice. The skeletal abnormalities, especially the rachitic rosary-like structures in the ribs and unclosed large fontanelle, were reminiscent of rickets.

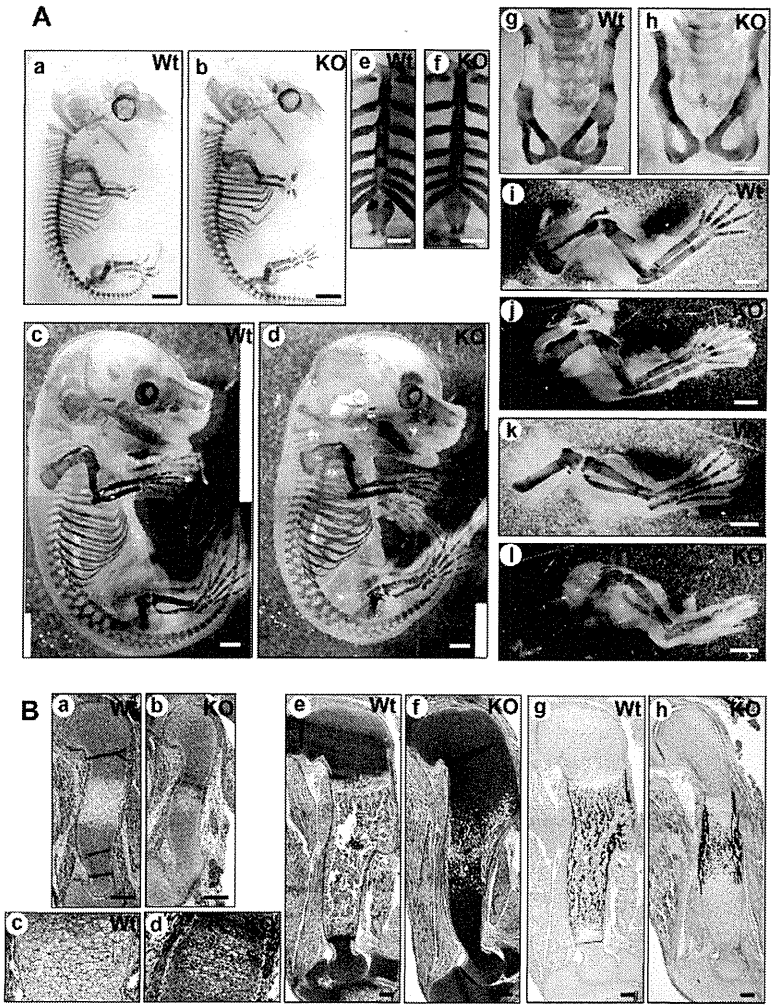

Fig. 2. Impaired chondrocyte hypertrophy in SIK3-deficient mouse embryos. (**A**) Wild-type and SIK3-deficient (KO) skeletons stained with Alizarin Red and Alcian Blue at E14.5 (a,b), E15.5 (c,d) and E18.5 (e-l): whole skeleton (a-d), sternum (e,f), pelvis (g,h), forelimb skeleton (i,j) and hindlimb skeleton (k,l). (**B**) Histological sections from wild-type and SIK3-deficient embryos stained with Safranin O, Fast Green and Iron Hematoxylin (a-f) or with von Kossa and Eosin (g,h) at E14.5 (a-d) and E18.5 (e-h). Scale bars: 1 mm in A; 200 μm in B.

In addition, SIK3 expression was detected in the kidney and liver, in which the effects of SIK3 deletion were also marked (T.U., Y. Itoh, O. Hatano, A. Kumagai, M. Sanosaka, T. Sasaki, S.S., J. Doi, K. Tatsumi, K. Mitamura et al., unpublished). Renal disorders produced by physical damage or chemical treatment sometimes induce osteomalacia, accompanied by low calcium and/or low phosphorus levels in the serum. Therefore, we measured the concentrations of calcium and phosphorus in the serum, and found that both were almost normal in SIK3-deficient mice (supplementary material Fig. S3). Thus, we excluded the possibility that the skeletal abnormalities of SIK3-deficient mice were due to impaired metabolism of phosphorus or calcium.

Accumulation of cartilage in SIK3-deficient mice

To further investigate the bone malformation in SIK3-deficient mice, we histologically analyzed the interior of the bones of 3-month-old (rib) or 4-month-old (other bones) mice. Safranin O staining revealed marked cartilage accumulation in most of the bones of SIK3-deficient mice. In the sternum, the cartilage region did not separate, and there was absolutely no bone marrow space (Fig. 1Ba,b). In the spine, expanded cartilage tissue and a malformed intervertebral disk were found (Fig. 1Bc,d). SIK3-deficient ribs were half filled with cartilage (Fig. 1Be,f). The epiphysis and metaphysis of the limb bones of SIK3-deficient mice were filled with cartilage bulk and displayed small secondary ossification centers (Fig. 1Bg-j, supplementary material Fig. S4C,D), whereas a well-differentiated secondary ossification center was developed in wild-type mice by 3 weeks of age. Although separation between the articular cartilage and the growth plate cartilage was found in 4-month-old SIK3-deficient mice, the secondary ossification center was not well developed even by 8 months of age (supplementary material Fig. S4C-L). In the articular cartilage of SIK3-deficient mice, the zone below the tidemark was thickened. The Safranin O staining intensity and cell morphology in the zone above the tidemark of articular cartilage were similar in SIK3-deficient and wild-type mice (Fig. 1Bk). Collectively, these findings indicate that impaired chondrocyte metabolism was fundamental to the skeletal abnormalities of SIK3-deficient mice.

Impaired chondrocyte hypertrophy in SIK3-deficient embryos

To pinpoint the onset of the skeletal abnormalities in SIK3-deficient mice we next surveyed skeletal development at various embryonic stages by Alcian Blue/Alizarin Red staining. Neither skeletal malformation nor homeotic transformation was observed in SIK3-deficient embryos at E14.5, indicating that *Sik3* gene deletion did not affect the chondrogenic commitment of mesenchymal cells or skeletal patterning (Fig. 2Aa,b). In wild-type mouse embryos, bone mineralization was indicated by Alizarin Red staining in several skeletal elements by E15.5. Compared with wild-type embryos, delayed mineralization of the ribs, the long bones in the limbs and cervical bones was observed in SIK3-

deficient embryos at E15.5 (Fig. 2Ac,d). By E18.5, the mineralization at most skeletal elements that are developed through endochondral bone formation had progressed in wild-type embryos. By contrast, SIK3-deficient embryos displayed delayed bone mineralization. The sternum and vertebrae remained uncalcified (Fig. 2Ae-h). The mineralized regions at the pelvis (Fig. 2Ag,h), the scapula and the long bones of the forelimb and hindlimb (Fig. 2Ai-l) were markedly reduced in SIK3-deficient embryos as compared with wild-type embryos at E18.5. By contrast, the shape and size of the cartilage in the epiphyseal and metaphysial regions of the limbs were almost normal in SIK3-deficient embryos (Fig. 2B). In spite of the reduced mineralization, the length of the long bones in the limbs was almost the same in SIK3-deficient and wild-type embryos (supplementary material Fig. S5A). Reflecting this finding, the body size of newborns was indistinguishable between genotypes (supplementary material Fig. S1C). After birth, bone elongation in the SIK3-deficient mice was restricted, and the length of the long bones in the limbs was obviously shortened at 6 weeks of age (supplementary material Fig. S5A).

A further histological analysis revealed a definitive primary defect of the cartilage in SIK3-deficient embryos. A cluster of well-differentiated hypertrophic chondrocytes is initially observed at the center of the humerus in wild-type embryos at E14.5. By contrast, only a few partially differentiated chondrocytes were observed at the center of the humerus in SIK3-deficient embryos at E14.5 (Fig. 2Ba-d). Therefore, we speculated that a disturbance of chondrocyte hypertrophy was the point at which SIK3 deficiency affected skeletal development. At E18.5, the first ossification center is well formed in the central region and the cartilage region is restricted at both ends in the wild-type mouse humerus. By contrast, the humerus of SIK3-deficient embryos was almost completely filled with cartilage tissue and the small first ossification center was barely recognizable (Fig. 2Be,f).

To characterize the cartilage tissue that accumulated in the humerus of SIK3-deficient embryos, we examined the expression of several structural markers of cartilage (types I, II and X collagen) at E18.5. We confirmed that the accumulated cartilage tissue was type I collagen-negative and type II collagen-positive, indicating that the tissue was bona fide cartilage tissue, consistent with the intense Safranin O staining (supplementary material Fig. S6A). Type X collagen, a hypertrophic structural marker, was only weakly detected at the center of the SIK3-deficient humeri, reflecting a disturbance in chondrocyte hypertrophy (supplementary material Fig. S6A). A further analysis based on cell morphology revealed that the round chondrocyte zone was of normal length but that there was an extended flat columnar chondrocyte zone and post-flat chondrocyte zone in SIK3-deficient compared with wild-type humeri at E18.5 (supplementary material Fig. S7). By assessing the expression of PCNA, it was confirmed that most of the accumulated flat chondrocytes were in a proliferative state (supplementary material Fig. S8).

In spite of the disruption of chondrocyte hypertrophy, significant mineralization, as confirmed by von Kossa staining, was observed at the bone collar of the humerus in SIK3-deficient embryos at E18.5, and it was apparently thicker than that in wild-type embryos (Fig. 2Bg,h). A real-time RT-PCR analysis showed that the genes encoding the mineralization factors ANK and ENPP were expressed at E18.5 in SIK3-deficient humerus, although the expression levels were slightly reduced (supplementary material Fig. S5B). The expression levels of the genes encoding the vascularization factors VEGF and VEGFR and the hypoxia inducible factors HIF1α and HIF2α (EPAS1 – Mouse Genome Informatics) were similar in wild-type and SIK3-deficient humeri (supplementary material Fig. S5B). A similar phenomenon has been reported in *Sox9* transgenic embryos, in which chondrocyte hypertrophy was suppressed (Akiyama et al., 2004; Hattori et al., 2010). These findings suggest that there is a system that compensates for bone mineralization in cases of disruption of endochondral skeletal development. We also performed the TUNEL assay to determine whether apoptosis was occurring in the accumulating cartilage tissue in SIK3-deficient embryos and juvenile mice. Few TUNEL-positive cells were detected in the accumulating cartilage tissue of E18.5 and juvenile specimens (supplementary material Fig. S8), suggesting that the accumulated chondrocytes in SIK3-deficient mice were not actively removed but remain alive until entry into hypertrophy upon differentiation.

Although the SIK3-deficient humerus was filled with chondrocytes at E18.5 (Fig. 2Be,f), first and secondary ossification centers were eventually formed (supplementary material Fig. S4) and mineralization occurred (Fig. 1A) with increasing age. These results suggested that the chondrocyte hypertrophy program was diminished rather than completely abolished. In order to clarify whether the post-hypertrophic program was still functional, we analyzed the expression of MMP13, a post-hypertrophic marker (Mitchell et al., 1996), and of SP7 (osterix), an osteogenesis marker (Nakashima et al., 2002), in juvenile epiphyseal tibia specimens. Consistently, expression of these markers was observed, although their expression patterns were somewhat disorganized compared with the wild-type tissues (supplementary material Fig. S6B). Taken together, it was concluded that the major effect of SIK3 deficiency on skeletal development was disruption of chondrocyte hypertrophy.

Expression of SIK3 in hypertrophic chondrocytes

Based on a histological analysis, we revealed that SIK3 deficiency results in the disruption of chondrocyte hypertrophy (Figs 1, 2). To address the endogenous SIK3 expression pattern in cartilage tissue, we performed immunofluorescent staining for SIK3 in wild type. Consistent with the histological results, endogenous SIK3 was detected in both prehypertrophic and hypertrophic chondrocytes, and it was localized in the cytoplasm of cells in the humerus at E18.5 (Fig. 3Aa,b), scapula at E15.5 (Fig. 3Ac,d) and growth plate of the knee at 3 weeks of age (Fig. 3Ae,f).

Previously, it was revealed that HDAC4 and MEF2C are central regulators of chondrocyte hypertrophy and skeletogenesis and that HDAC4 functions as a transcriptional repressor for MEF2C and RUNX2 (Vega et al., 2004; Arnold et al., 2007). Other studies have also reported interactions between SIK1/2 and HDACs (van der Linden et al., 2007; Takemori et al., 2009). We therefore hypothesized that SIK3 might exert its effect via HDAC4 to regulate the activities of MEF2C and RUNX2 in chondrocyte hypertrophy. To evaluate this hypothesis, we first immunohistochemically analyzed the expression of SOX9, HDAC4 and MEF2C (as a representative target of HDAC4) in the wild-type humerus at E15.5 (Fig. 3B). As previously reported, SOX9 was detected in the proliferative and in some of the prehypertrophic chondrocytes and was undetectable in hypertrophic chondrocytes (Fig. 3Bc,d). Expression of MEF2C and HDAC4 was detected in both the prehypertrophic and hypertrophic chondrocyte regions (Fig. 3Be-h). The expression of SIK3 was exclusive to cells that also expressed SOX9 and was similar to that of HDAC4 (Fig. 3Bi,j).

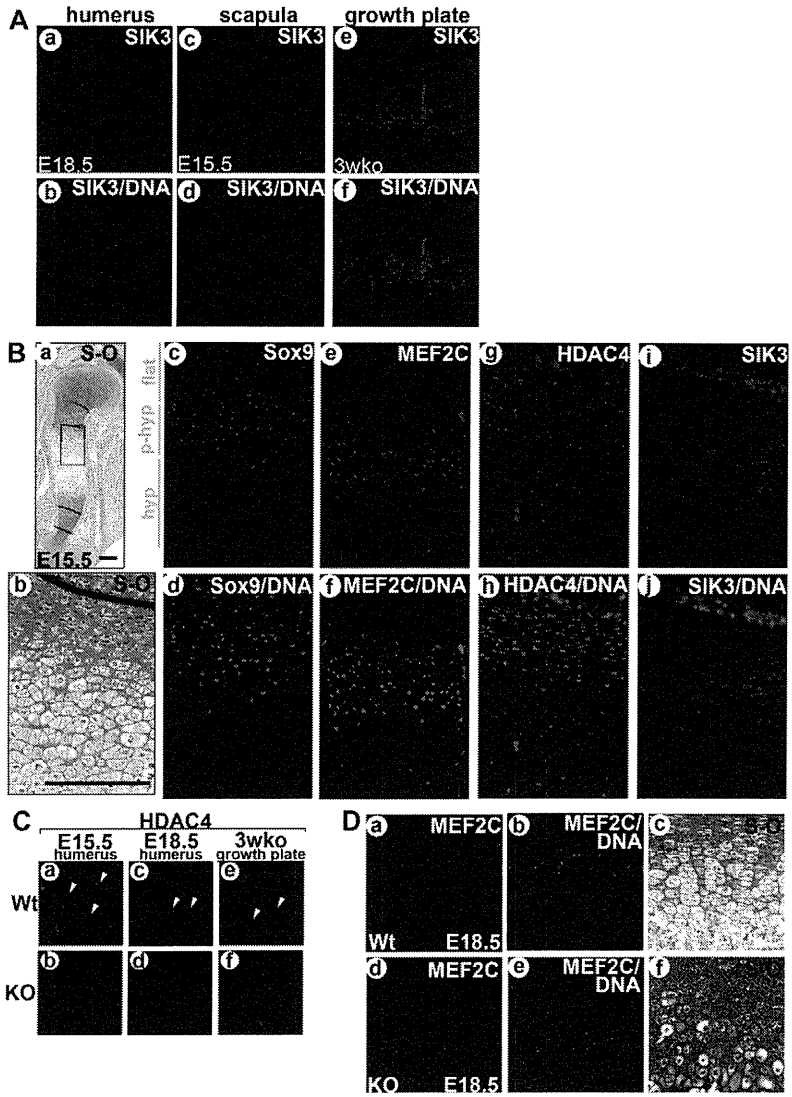

Fig. 3. Expression patterns of SIK3 and chondrocyte hypertrophic factors. (**A**) Immunofluorescent staining for SIK3 (red) in the humerus (a,b), scapula (c,d) and growth plate of the proximal tibia of 3-week-old (e,f) wild-type mice. Nuclei were counterstained with Hoechst 33342 (blue). SIK3 expression was detected in prehypertrophic and hypertrophic chondrocytes and was localized in the cytoplasm in all tissues analyzed. (**B**) A comparison of the expression patterns of SIK3 and chondrocyte hypertrophic factors in the humerus of wild-type embryos (E15.5). Bright-field views of a section stained with Safranin O, Fast Green and Hematoxylin are shown (a,b). Serial sections were stained with anti-SOX9 (c,d), anti-MEF2C (e,f), anti-HDAC4 (g,h) or anti-SIK3 (i,j) antibodies and an Alexa Fluor-conjugated secondary antibody. Scale bars: 200 μm. (**C**) Immunofluorescent staining for HDAC4 in the humerus at E15.5 (a,b) and E18.5 (c,d) and in the growth plate of the proximal tibia at 3 weeks of age (e,f) of wild-type (a,c,e) and SIK3-deficient (b,d,f) mice. Arrowheads indicate cells in which HDAC4 was excluded from the nucleus. However, HDAC4 persisted in the nucleus in the SIK3-deficient specimens. (**D**) Immunofluorescent staining for MEF2C in the humerus at E18.5 in wild-type (a,b) and SIK3-deficient (d,e) embryos. Semi-serial sections were stained with Safranin O, Fast Green and Hematoxylin (c,f).

We also found that there was a shift in the subcellular localization of HDAC4 to the cytoplasm in hypertrophic chondrocytes, where the expression of MEF2C was strong in the nuclei. The translocation of HDAC4 was observed at the hypertrophic chondrocyte zone in the humerus of E15.5 and E18.5 embryos and in the growth plate of 3-week-old wild-type mice (Fig. 3C). By contrast, HDAC4 translocation to the cytoplasm was seldom observed in chondrocytes at the corresponding region in SIK3-deficient embryos and mice. However, although the location was not synchronized, significant MEF2C-positive cells were observed at the edge of the accumulated cartilage in SIK3-deficient humeri, despite the fact that chondrocyte hypertrophy had not progressed (Fig. 3Dd-f). We therefore concluded that the HDAC4 remaining in the nuclei of the SIK3-deficient chondrocytes continued to repress MEF2C activity, resulting in the blockage of chondrocyte hypertrophy. Taken together, these data indicated that SIK3 is required for HDAC4 translocation to the cytoplasm during chondrocyte hypertrophy.

SIK3 forms a complex with HDAC4 to regulate its subcellular localization

To address how SIK3 regulates the subcellular localization of HDAC4, we performed a co-immunoprecipitation assay to determine whether they form a complex. The co-immunoprecipitation assay with knee lysates from 2-week-old mice indicated that a complex was indeed formed between HDAC4 and SIK3 (Fig. 4A). To further analyze the regulation of HDAC4 by SIK3 in vitro, HA-tagged HDAC4 and SIK3 expression vectors were co-transfected into 293FT cells, lysed, and assayed with an anti-HA antibody. This confirmed that HDAC4 and SIK3 form a complex (Fig. 4B). Using this system, we explored the binding domains of SIK3 and HDAC4 required for complex formation, and identified the kinase domain (amino acids 1-270) of SIK3 and the central region (amino acids 351-620) of HDAC4 as binding domains (supplementary material Fig. S9).

We next examined whether this interaction affects the subcellular localization of HDAC4. To monitor HDAC4 localization, an EGFP-tagged HDAC4 expression vector was transfected into 293FT cells with or without the SIK3 expression vector, and GFP was observed by fluorescence microscopy. In agreement with the expression pattern of endogenous SIK3 in hypertrophic chondrocytes (Fig. 3B), the overexpressed SIK3 was detected in the cytoplasm (Fig. 4C). When GFP-HDAC4 was overexpressed alone, GFP fluorescence was observed in the nucleus (Fig. 4D, upper panel). By contrast, when SIK3 was co-expressed, GFP fluorescence was observed in the cytoplasm (Fig. 4D, bottom panels). These results indicated that SIK3 can alter the localization

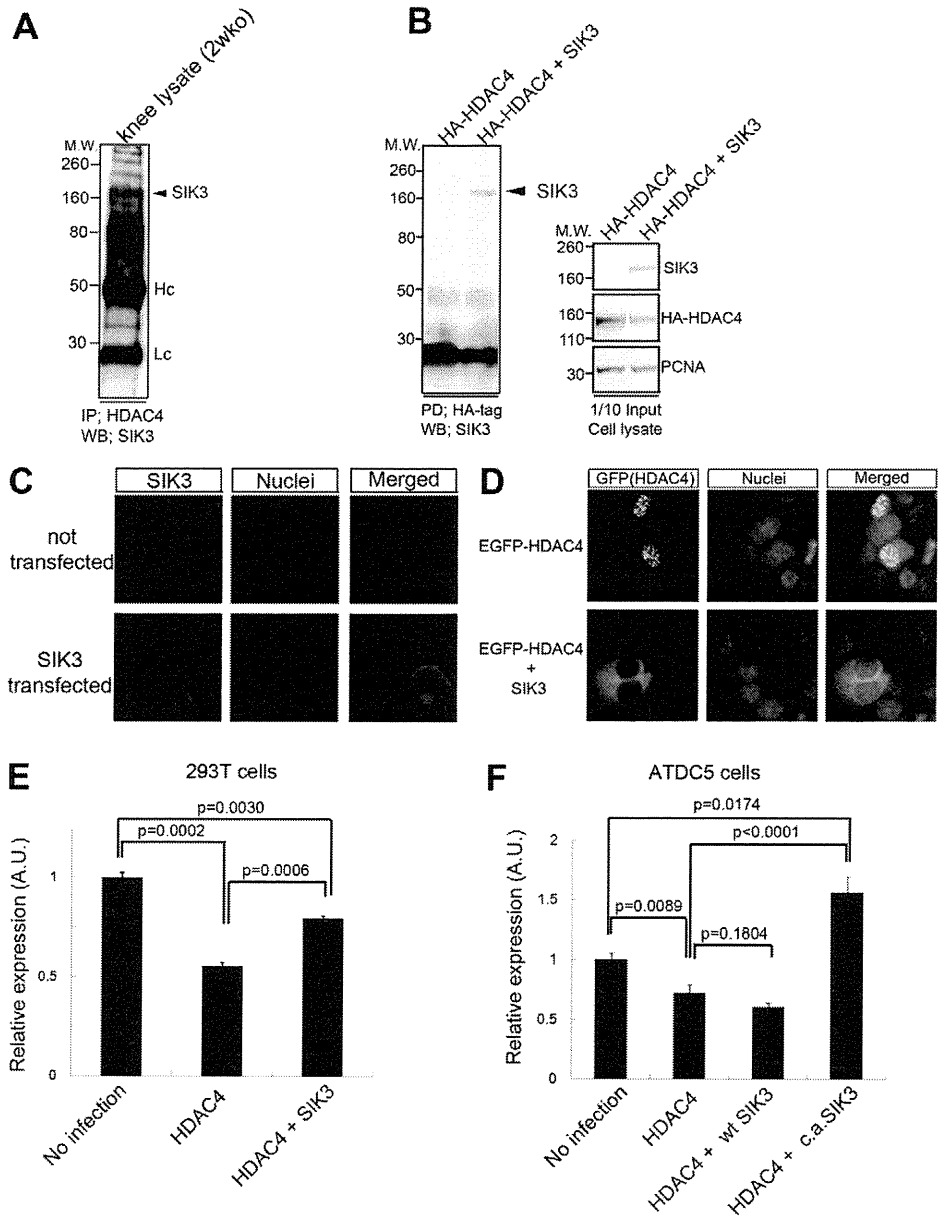

Fig. 4. Interaction of SIK3 with HDAC4 regulates its subcellular localization. (**A**) Co-immunoprecipitation of SIK3 with HDAC4. Knee tissue from 2-week-old mice was lysed and endogenous HDAC4 immunoprecipitated. Co-immunoprecipitated SIK3 was detected. Hc, IgG heavy chain; Lc, IgG light chain. (**B**) Pulldown assay of SIK3 with HA-HDAC4. 293FT cells were transiently transfected with expression vectors carrying SIK3 and HA-tagged HDAC4. Pulled-down samples (PD) and whole cell lysates (input) were subjected to SDS-PAGE followed by immunoblotting with the indicated antibodies. Left and right panels show the pulldown assay and the transiently expressed proteins, respectively. PCNA was monitored as a loading control. (**C**) SIK3 immunofluorescence. 293FT cells were transiently transfected with a SIK3 expression vector and stained 24 hours after transfection using an anti-SIK3 antibody followed by an Alexa Fluor-conjugated secondary antibody. A SIK3 signal was detected in the cytoplasm of transfected cells, whereas there was no substantial signal in non-transfected cells. (**D**) Translocation of HDAC4 by SIK3. A GFP-HDAC4 expression vector was transfected with or without a SIK3 expression vector into 293FT cells. When EGFP-HDAC4 was transfected alone, GFP fluorescence was detected in the nuclei (top panels). When EGFP-HDAC4 and SIK3 were co-transfected, GFP fluorescence was detected in the cytoplasm (bottom panels). Nuclei were counterstained with Hoechst 33342. (**E**) MEF2C transcriptional activity in 293FT cells. 293FT cells were transiently transfected with a MEF2C-luciferase reporter plasmid and an expression vector encoding MEF2C without (basal control) or with expression vectors for HDAC4 and/or wild-type SIK3. The luciferase activity was measured 48 hours after transfection. (**F**) MEF2C transcriptional activity in ATDC5 cells. ATDC5 cells were transiently transfected with a MEF2C-luciferase reporter plasmid and an expression vector encoding MEF2C without (basal control) or with expression vectors for HDAC4 and/or wild-type SIK3, or with a constitutively active form of SIK3 (T163E, S494A). Error bars indicate s.d.

of HDAC4 from the nucleus to the cytoplasm. We also performed a MEF2C luciferase reporter assay to monitor whether the HDAC4 translocation induced by SIK3 might relieve MEF2C activity from suppression by HDAC4. When MEF2C was co-expressed with HDAC4, the MEF2C reporter activity was suppressed. In addition, when SIK3 was co-overexpressed recovery of the luciferase activity was observed, although the recovery was not complete (Fig. 4E). In ATDC5 cells, a prechondrogenic cell line, constitutively active forms of SIK3 (T163E, S494A), but not wild-type SIK3, showed HDAC4 inhibitory activity, suggesting that

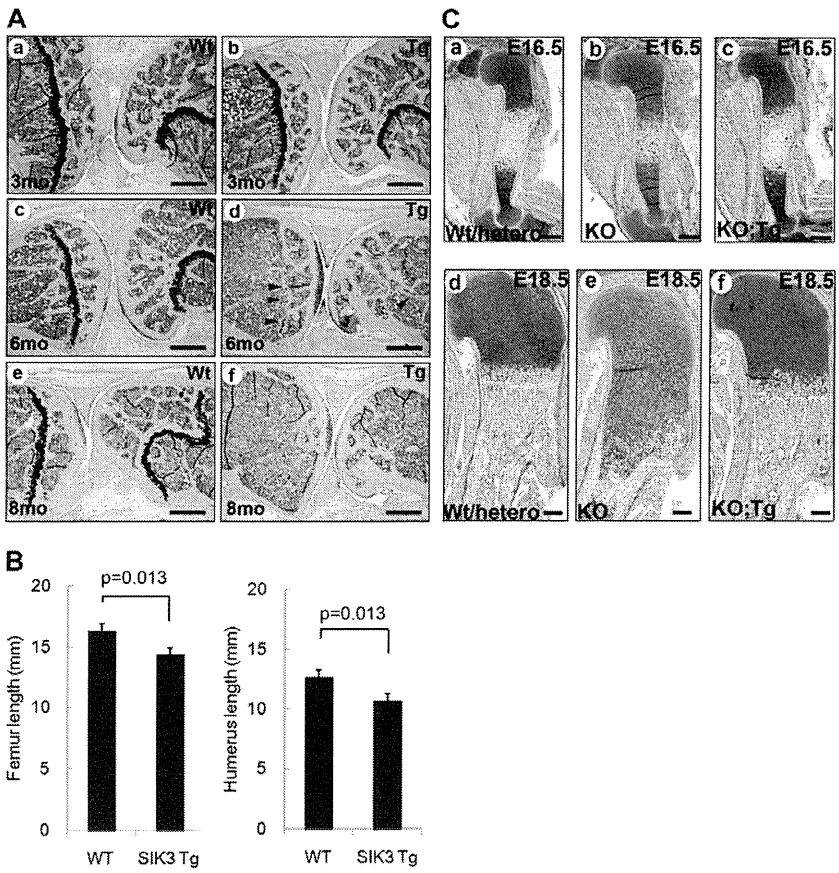

Fig. 5. Effects of forced expression of SIK3 in cartilage tissue. (**A**) Histological sections of the knee joint of wild-type and *Col11a2-hSIK3* transgenic mice stained with Safranin O and Fast Green. At 3 months of age, the growth plate of the transgenic mice appeared normal (a,b). By 6 months, the growth plate was starting to disappear (c,d) and by 8 months of age it had completely disappeared and the spongy bone was also starting to disappear (e,f). By contrast, the growth plates persisted in wild-type mice until they were 8 months of age. Arrowheads indicate the residual growth plates. (**B**) A comparison of the length of femur and humerus between wild-type and *hSIK3* transgenic (Tg) mice at 6 months of age. The *hSIK3* transgenic mice had shortened long bones. Error bars indicate s.d. (**C**) Transgenic rescue of SIK3. A $Sik3^{+/-}$ female mouse was mated with a $Sik3^{+/-}$; *Col11a2-hSIK3* transgenic male mouse and the embryos were dissected at E16.5 (a-c) or E18.5 (d-f). Chondrocyte accumulation in the SIK3-deficient proximal humerus was substantially restored by the *Col11a2-hSIK3* transgene. Scale bars: 500 μm in A; 200 μm in C.

ATDC5 cells lack factors that are required for the activation of SIK3 (Fig. 4F). Overall, these findings indicated that SIK3 anchors HDAC4 in the cytoplasm, thereby allowing MEF2C to be active.

Forced SIK3 expression in cartilage causes closure of the growth plate in adulthood

The expression of SIK3 in hypertrophic chondrocytes and impaired chondrocyte hypertrophy in SIK3-deficient embryos and mice indicate that SIK3 is indispensable for chondrocyte hypertrophy. We generated transgenic mice overexpressing human *SIK3* (*hSIK3*) specifically in chondrocytes under the control of *Col11a2* promoter/enhancer sequences (Tsumaki et al., 1996; Murai et al., 2008; Hiramatsu et al., 2011) to confirm the role of SIK3 in cartilage by a gain-of-function approach and to clarify that the phenotype of bone malformation in SIK3-deficient mice was really due to the cartilage tissue.

We previously demonstrated that GFP fluorescence driven by this system is detected only in the cartilage tissue during embryogenesis (Hiramatsu et al., 2011) and in both the articular and growth plate cartilage in adulthood (data not shown). To confirm the expression of the *hSIK3* transgene using this system, costal cartilage was harvested from postnatal pups at the P2 stage and subjected to SDS-PAGE, followed by immunoblotting with a SIK3 antibody (supplementary material Fig. S10). Although a dramatic effect of SIK3 overexpression was not observed during embryogenesis or during the juvenile period in *Col11a2-hSIK3* transgenic mice, we did observe the disappearance of the growth plate in the hind limbs with aging (Fig. 5A).

Generally, the growth plate is thought to comprise continually metabolizing chondrocytes, which are balanced in proliferation and differentiation (i.e. hypertrophy). Based on our findings, we speculated that the disappearance of the growth plate in cartilage-specific *hSIK3* transgenic mice occurred because the overexpressed SIK3 slightly accelerated the differentiation of chondrocytes at the growth plate, leading to chronic and excessive usage of chondrocytes and resulting in loss of the growth plate structure in older mice. Consistent with this hypothesis, the length of the long bones was reduced at 6 months of age (Fig. 5B) and the spongy bone structure was also beginning to disappear by 8 months of age in the *Col11a2-hSIK3* transgenic mice (Fig. 5A). Thus, we concluded that the disappearance of the growth plate in cartilage-specific *hSIK3* transgenic mice was a predictable phenotype for the gain-of-function approach for SIK3. In addition, the *Col11a2-hSIK3* transgenic/SIK3-deficient offspring displayed efficient rescue of the impaired chondrocyte hypertrophy phenotype at E16.5 (Fig. 5C, top panels) and at E18.5 (Fig. 5C, bottom panels). Nevertheless, despite the restoration of the bone phenotype, the lethality of SIK3 deficiency for newborn mice was not recovered, suggesting that bone deformity is not the primary cause of their postnatal death. Taken together, these results confirmed that the role of SIK3 in chondrocytes is to induce the progression of chondrocyte hypertrophy and that the impaired skeletal development of SIK3-deficient mice is due to the cartilage tissue.

DISCUSSION

Our study revealed that SIK3 is a crucial regulator of chondrocyte hypertrophy and identified the transcriptional regulator, HDAC4, as a target of SIK3 in chondrogenesis. SIK3-deficient mice displayed multiple phenotypes, including bone malformation with dwarfism, and these were concluded to be due to impaired chondrocyte hypertrophy. The abnormalities of the bone that develops via endochondral bone formation in

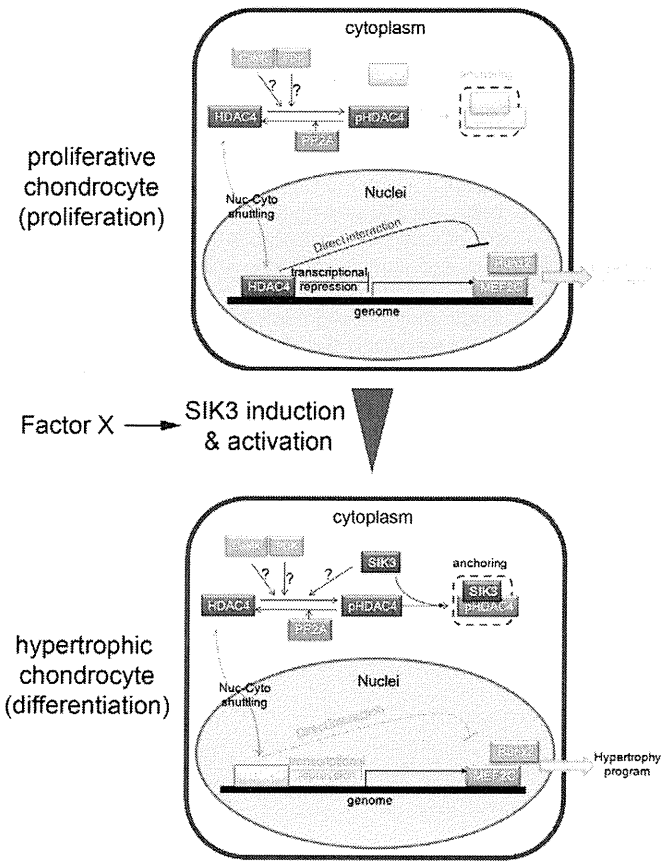

Fig. 6. Model depicting the role of SIK3 in chondrocyte hypertrophy. (Top) When SIK3 is absent, HDAC4 remains in the nucleus and epigenetically and mechanically represses MEF2C. (Bottom) Once SIK3 is induced, SIK3 binds to HDAC4 and anchors it in the cytoplasm, thereby allowing MEF2C to become active in the nucleus and facilitating the progression of the chondrocyte hypertrophic program. Question marks indicate possible phosphorylation activities opposing to PP2A, but not tested.

SIK3-deficient embryos were similar to those of cartilage-specific *Hdac4* transgenic embryos (Vega et al., 2004). Furthermore, our results showed that SIK3 forms a complex with HDAC4 and anchors it in the cytoplasm, thereby relieving MEF2C from transcriptional repression by HDAC4 in the nuclei. In conclusion, the regulation of HDAC4 by SIK3 is a crucial mechanism for the progression of chondrocyte hypertrophy during skeletal development (Fig. 6).

Expression of SIK3 in chondrocytes

SIK3-deficient mice were generated to better understand the physiological role of SIK3. We identified bone deformity with dwarfism as one of the phenotypes of SIK3-deficient mice. We found strong expression of SIK3 from prehypertrophic to hypertrophic chondrocytes during chondrogenesis and in the postnatal growth plate, suggesting the importance of SIK3 in chondrocyte hypertrophy. Indeed, SIK3-deficient embryos displayed impaired chondrocyte hypertrophy, which resulted in bone abnormalities. Furthermore, cartilage-specific *hSIK3* transgenic mice showed unnatural closure of the growth plate. As a result of our gain-of-function approach, it was demonstrated that the expression of additional SIK3 hastened chondrocyte hypertrophy and led to the depletion of non-hypertrophic chondrocytes, which are normally necessary to maintain the growth plate structure. Although the SIK3 expression pattern was consistent with its function in chondrocytes, further questions also arose. For example, it is unclear how and which transcription factor(s) regulate SIK3 expression in chondrocytes. So far, there have been few studies, but we intend to address this question in future studies to obtain a deeper understanding of the mechanism responsible for endochondral bone development.

Molecular mechanisms by which SIK3 exerts its activity in chondrocytes

One of the major findings of this study is that SIK3 regulates the subcellular localization of HDAC4, a negative transcriptional regulator of MEF2C and RUNX2 activity during chondrocyte differentiation, i.e. hypertrophy. For the first time, we revealed that SIK3 was strongly expressed from prehypertrophic to hypertrophic chondrocytes, in which HDAC4 was also expressed. In addition, we found that HDAC4 localization was shifted to the cytoplasm in wild-type chondrocytes, but that this seldom occurred in SIK3-deficient chondrocytes. In response to HDAC4 translocation, wild-type chondrocytes began hypertrophy. By contrast, chondrocyte hypertrophy was severely inhibited in spite of sufficient MEF2C expression in SIK3-deficient cartilage tissue. However, flat chondrocytes continued proliferating, maintaining their columnar structure and causing chondrocyte accumulation during development. These results suggested that SIK3 is required for proper chondrocyte hypertrophy and that its role is to change the subcellular localization of HDAC4 from the nucleus to the cytoplasm during chondrocyte differentiation.

Several studies have reported that SIK1 and SIK2 directly regulate HDACs (van der Linden et al., 2007; Takemori et al., 2009). Fly SIK3 (the homolog of mouse SIK2) has recently been shown to sequester HDAC4 in the cytoplasm and to regulate the energy balance in the *Drosophila* fat body (Wang et al., 2011). We therefore hypothesized that mouse SIK3 directly regulates HDAC4. Indeed, we confirmed that SIK3 and HDAC4 form a stable complex by performing a pulldown assay. We found that the subcellular localization of SIK3 in chondrocytes in vivo was the cytoplasm. In fact, we did not find any nuclear localization signal in its sequence, and the SIK3 that was ectopically expressed in the 293FT cells was detected in the cytoplasm. By contrast, HDAC4 was detected in both the cytoplasm and the nucleus in proliferative chondrocytes, whereas it was localized in the cytoplasm in hypertrophic chondrocytes. It is also known that HDAC4 shuttles between the cytoplasm and nucleus. Considering these findings, it appears that when SIK3 is present in the cytoplasm, HDAC4 is anchored there. Consistent with this idea, we demonstrated that GFP-HDAC4, which was localized in nuclei when expressed alone, was localized in the cytoplasm when SIK3 was co-expressed in 293FT cells. Furthermore, anchoring HDAC4 to the cytoplasm by SIK3 co-expression allowed reactivation of the MEF2C repressed by HDAC4 in nuclei in vitro.

It is thought that the role of SIK3 during chondrocyte differentiation is to exclude HDAC4 from the nucleus, thereby allowing MEF2C to be transcriptionally active in the nucleus to induce progression of the chondrocyte hypertrophy program. We found that constitutively active forms of SIK3 (T163E, S494A), but not wild-type SIK3, inhibited HDAC4 activity in ATDC5 cells, suggesting the presence of other factors that are needed for SIK3 activation. Previously, LKB1 (STK11 – Mouse Genome

Informatics) was shown to be an activator of SIK3, and it phosphorylates SIK3 at Thr163 (Lizcano et al., 2004), raising the possibility that LKB1 might be a regulator of SIK3. The mild cartilage phenotype in *Col11a2-hSIK3* transgenic mice compared with that in *Mef2c* transgenic or HDAC4-deficient mice might indicate that the presence of additional factors is required for the activation of *Sik3* in chondrocytes. In the *hSIK3* transgenic growth plate, we did not see obvious changes in HDAC4 localization (data not shown) in spite of the presence of growth plate abnormalities. A possible explanation for this discrepancy is that the changes might have been too faint to be detected by immunofluorescence microscopy. It is also possible that other undefined mechanisms act downstream of SIK3, in parallel to HDAC4. *Col11a2-hSIK3* transgenic mice showed early closure of the growth plates. Growth plate disappearance has been reported in mice in which IHH (Maeda et al., 2007) and the PTH/PTHrP receptor (Hirai et al., 2011) were deleted postnatally. Because IHH and PTH/PTHrP regulate chondrocyte hypertrophy, SIK3 might be localized and controlled by these signaling molecules during the progression of chondrocyte hypertrophy. The SIK3-deficient cartilage phenotype was rescued by *Col11a2-hSIK3* transgene expression, suggesting that the impaired skeletal development in SIK3-deficient mice is primarily due to the cartilage tissue. It is also possible that changes in cholesterol metabolism and malnourishment phenotypes in the SIK3-deficient mice (T.U., Y. Itoh, O. Hatano, A. Kumagai, M. Sanosaka, T. Sasaki, S.S., J. Doi, K. Tatsumi, K. Mitamura et al., unpublished) affect chondrocyte differentiation, as cholesterol signaling stimulates chondrocyte hypertrophy (Woods et al., 2009) and because malnourishment phenotypes, including lipodystrophy, hypolipidemia and hypoglycemia, should affect skeletal growth. The SIK3-deficient bone phenotypes displayed at adulthood in this study might have occurred due to a combination of direct SIK3 disruption in chondrocytes and indirect SIK3 disruption due to metabolic changes.

Previously, PP2A was proposed as a regulator of HDAC4 by localizing it in the nucleus, thereby prohibiting chondrocyte hypertrophy (Kozhemyakina et al., 2009). However, no opposing mechanisms have been suggested. Our present findings are therefore the first to indicate that SIK3 has an antagonistic role in HDAC4 regulation during chondrogenesis. Although we did not perform an in-depth analysis of the underlying mechanism(s) of action in this study, we did observe impaired skull bone development, which occurs through membranous ossification, suggesting that SIK3 is involved in membranous ossification as well. Further studies are needed to better understand the functions of SIK3 in skeletal development, including the generation of conditional knockout mice.

Acknowledgements
We thank Dr Gen Nishimura for advice on manuscript preparation; Dr James Hsieh for providing instructions for the immunoprecipitation assay; Ms Mari Shinkawa for technical assistance; Drs Hidetatsu Outani, Hirohiko Yasui, Yoshiki Minegishi, Minoru Okada, Jun Yoshino and Takao Hirai for discussions and suggestions; and Dr Kazuyuki Itoh for support.

Funding
This study was supported in part by the Japan Science Technology Agency (JST); Core Research for Evolutional Science and Technology (CREST) (to N.T.); Ministry of Education, Culture, Sports, Science and Technology (MEXT) [Scientific Research Grant No. 21390421 to N.T.]; and the Natural Scientists and the Strategic Project to Support the Formation of Research Bases at Private Universities (to H.T.).

Competing interests statement
The authors declare no competing financial interests.

Supplementary material
Supplementary material available online at
http://dev.biologists.org/lookup/suppl/doi:10.1242/dev.072652/-/DC1

References
Akiyama, H., Chaboissier, M. C., Martin, J. F., Schedl, A. and de Crombrugghe, B. (2002). The transcription factor Sox9 has essential roles in successive steps of the chondrocyte differentiation pathway and is required for expression of Sox5 and Sox6. *Genes Dev.* **16**, 2813-2828.
Akiyama, H., Lyons, J. P., Mori-Akiyama, Y., Yang, X., Zhang, R., Zhang, Z., Deng, J. M., Taketo, M. M., Nakamura, T., Behringer, R. R. et al. (2004). Interactions between Sox9 and beta-catenin control chondrocyte differentiation. *Genes Dev.* **18**, 1072-1087.
Arnold, M. A., Kim, Y., Czubryt, M. P., Phan, D., McAnally, J., Qi, X., Shelton, J. M., Richardson, J. A., Bassel-Duby, R. and Olson, E. N. (2007). MEF2C transcription factor controls chondrocyte hypertrophy and bone development. *Dev. Cell* **12**, 377-389.
Hattori, T., Muller, C., Gebhard, S., Bauer, E., Pausch, F., Schlund, B., Bosl, M. R., Hess, A., Surmann-Schmitt, C., von der Mark, H. et al. (2010). SOX9 is a major negative regulator of cartilage vascularization, bone marrow formation and endochondral ossification. *Development* **137**, 901-911.
Hirai, T., Chagin, A. S., Kobayashi, T., Mackem, S. and Kronenberg, H. M. (2011). Parathyroid hormone/parathyroid hormone-related protein receptor signaling is required for maintenance of the growth plate in postnatal life. *Proc. Natl. Acad. Sci. USA* **108**, 191-196.
Hiramatsu, K., Sasagawa, S., Outani, H., Nakagawa, K., Yoshikawa, H. and Tsumaki, N. (2011). Generation of hyaline cartilaginous tissue from mouse adult dermal fibroblast culture by defined factors. *J. Clin. Invest.* **121**, 640-657.
Ikegami, D., Akiyama, H., Suzuki, A., Nakamura, T., Nakano, T., Yoshikawa, H. and Tsumaki, N. (2011). Sox9 sustains chondrocyte survival and hypertrophy in part through Pik3ca-Akt pathways. *Development* **138**, 1507-1519.
Karsenty, G., Kronenberg, H. M. and Settembre, C. (2009). Genetic control of bone formation. *Annu. Rev. Cell Dev. Biol.* **25**, 629-648.
Katoh, Y., Takemori, H., Horike, N., Doi, J., Muraoka, M., Min, L. and Okamoto, M. (2004). Salt-inducible kinase (SIK) isoforms: their involvement in steroidogenesis and adipogenesis. *Mol. Cell. Endocrinol.* **217**, 109-112.
Katoh, Y., Takemori, H., Lin, X. Z., Tamura, M., Muraoka, M., Satoh, T., Tsuchiya, Y., Min, L., Doi, J., Miyauchi, A. et al. (2006). Silencing the constitutive active transcription factor CREB by the LKB1-SIK signaling cascade. *FEBS J.* **273**, 2730-2748.
Komori, T., Yagi, H., Nomura, S., Yamaguchi, A., Sasaki, K., Deguchi, K., Shimizu, Y., Bronson, R. T., Gao, Y. H., Inada, M. et al. (1997). Targeted disruption of Cbfa1 results in a complete lack of bone formation owing to maturational arrest of osteoblasts. *Cell* **89**, 755-764.
Kozhemyakina, E., Cohen, T., Yao, T. P. and Lassar, A. B. (2009). Parathyroid hormone-related peptide represses chondrocyte hypertrophy through a protein phosphatase 2A/histone deacetylase 4/MEF2 pathway. *Mol. Cell. Biol.* **29**, 5751-5762.
Lefebvre, V. and Smits, P. (2005). Transcriptional control of chondrocyte fate and differentiation. *Birth Defects Res. C Embryo Today* **75**, 200-212.
Lizcano, J. M., Goransson, O., Toth, R., Deak, M., Morrice, N. A., Boudeau, J., Hawley, S. A., Udd, L., Makela, T. P., Hardie, D. G. et al. (2004). LKB1 is a master kinase that activates 13 kinases of the AMPK subfamily, including MARK/PAR-1. *EMBO J.* **23**, 833-843.
Maeda, Y., Nakamura, E., Nguyen, M. T., Suva, L. J., Swain, F. L., Razzaque, M. S., Mackem, S. and Lanske, B. (2007). Indian Hedgehog produced by postnatal chondrocytes is essential for maintaining a growth plate and trabecular bone. *Proc. Natl. Acad. Sci. USA* **104**, 6382-6387.
Mitchell, P. G., Magna, H. A., Reeves, L. M., Lopresti-Morrow, L. L., Yocum, S. A., Rosner, P. J., Geoghegan, K. F. and Hambor, J. E. (1996). Cloning, expression, and type II collagenolytic activity of matrix metalloproteinase-13 from human osteoarthritic cartilage. *J. Clin. Invest.* **97**, 761-768.
Murai, J., Ikegami, D., Okamoto, M., Yoshikawa, H. and Tsumaki, N. (2008). Insulation of the ubiquitous Rxrb promoter from the cartilage-specific adjacent gene, Col11a2. *J. Biol. Chem.* **283**, 27677-27687.
Nakashima, K., Zhou, X., Kunkel, G., Zhang, Z., Deng, J. M., Behringer, R. R. and de Crombrugghe, B. (2002). The novel zinc finger-containing transcription factor osterix is required for osteoblast differentiation and bone formation. *Cell* **108**, 17-29.
Ng, L. J., Wheatley, S., Muscat, G. E., Conway-Campbell, J., Bowles, J., Wright, E., Bell, D. M., Tam, P. P., Cheah, K. S. and Koopman, P. (1997). SOX9 binds DNA, activates transcription, and coexpresses with type II collagen during chondrogenesis in the mouse. *Dev. Biol.* **183**, 108-121.
Olsen, B. R., Reginato, A. M. and Wang, W. (2000). Bone development. *Annu. Rev. Cell Dev. Biol.* **16**, 191-220.

Takeda, S., Bonnamy, J. P., Owen, M. J., Ducy, P. and Karsenty, G. (2001). Continuous expression of Cbfa1 in nonhypertrophic chondrocytes uncovers its ability to induce hypertrophic chondrocyte differentiation and partially rescues Cbfa1-deficient mice. *Genes Dev.* **15**, 467-481.

Takeda, S., Chen, D. Y., Westergard, T. D., Fisher, J. K., Rubens, J. A., Sasagawa, S., Kan, J. T., Korsmeyer, S. J., Cheng, E. H. and Hsieh, J. J. (2006). Proteolysis of MLL family proteins is essential for taspase1-orchestrated cell cycle progression. *Genes Dev.* **20**, 2397-2409.

Takemori, H., Katoh Hashimoto, Y., Nakae, J., Olson, E. N. and Okamoto, M. (2009). Inactivation of HDAC5 by SIK1 in AICAR-treated C2C12 myoblasts. *Endocrine J.* **56**, 121-130.

Tsumaki, N., Kimura, T., Matsui, Y., Nakata, K. and Ochi, T. (1996). Separable cis-regulatory elements that contribute to tissue- and site-specific alpha 2(XI) collagen gene expression in the embryonic mouse cartilage. *J. Cell Biol.* **134**, 1573-1582.

van der Linden, A. M., Nolan, K. M. and Sengupta, P. (2007). KIN-29 SIK regulates chemoreceptor gene expression via an MEF2 transcription factor and a class II HDAC. *EMBO J.* **26**, 358-370.

Vega, R. B., Matsuda, K., Oh, J., Barbosa, A. C., Yang, X., Meadows, E., McAnally, J., Pomajzl, C., Shelton, J. M., Richardson, J. A. et al. (2004). Histone deacetylase 4 controls chondrocyte hypertrophy during skeletogenesis. *Cell* **119**, 555-566.

Wang, B., Moya, N., Niessen, S., Hoover, H., Mihaylova, M. M., Shaw, R. J., Yates, J. R., 3rd, Fischer, W. H., Thomas, J. B. and Montminy, M. (2011). A hormone-dependent module regulating energy balance. *Cell* **145**, 596-606.

Woods, A., James, C. G., Wang, G., Dupuis, H. and Beier, F. (2009). Control of chondrocyte gene expression by actin dynamics: a novel role of cholesterol/Ror-alpha signalling in endochondral bone growth. *J. Cell. Mol. Med.* **13**, 3497-3516.

Zhao, Q., Eberspaecher, H., Lefebvre, V. and De Crombrugghe, B. (1997). Parallel expression of Sox9 and Col2a1 in cells undergoing chondrogenesis. *Dev. Dyn.* **209**, 377-386.

Hypoxia Favors Maintenance of the Vascular Smooth Muscle Cell Phenotype in Culture

Naomi Yamasaki,[1] *Makoto Hirao,*[2] *Yoshitaka Kawato,*[1] *Kosuke Ebina,*[1] *Hiroki Oze,*[1] *Akihide Nampei,*[1] *Kenrin Shi,*[1] *Hideki Yoshikawa,*[1] *and Jun Hashimoto*[3]

[1]Department of Orthopaedics, Osaka University Graduate School of Medicine, Osaka, Japan

[2]Department of Orthopaedics, National Hospital Organization, Osaka-Minami Medical Center, Osaka, Japan; E-mail: *hira777@ommc-hp.jp*

[3]Department of Immune Disease, National Hospital Organization, Osaka-Minami Medical Center, Osaka, Japan

Received 14 May 2012; revised 29 May 2012; accepted 11 June 2012

Vascular smooth muscle cells (VSMCs) are derived from mesenchymal cells and differentiate into osteoblast-like cells at sites of atherosclerosis/arterial calcification [1–4]. VSMCs in the medial layer of arteries are normally protected from the high oxygen levels in arterial blood by the endothelium and intima. If the endothelium is damaged by atherosclerosis, however, VSMCs are possibly exposed to relatively high oxygen levels. Recently, we reported that relatively high oxygen tension promotes osteoblastic differentiation of mesenchymal stem cells [5]. Although certain stimuli, such as inorganic pyrophosphate, low-density lipoprotein levels, high glucose levels, and oxidative stress, can transform VSMCs into "calcifying vascular cells," that is, osteogenic cell [6–9], we hypothesized that exposure to excess oxygen also enhances the commitment of VSMCs to osteogenic differentiation, while keeping cells under a hypoxic condition maintains the VSMC phenotype. Immunohistochemical data showed diffuse expression of ORP150, a marker of hypoxia, in normal human arterial media, while its expression was decreased or abolished in calcified human arteries (Figure 1). Next, we used reverse transcription polymerase chain reaction (RT-PCR) and Western blot analysis to show that human VSMCs cultured under normoxic conditions (20% O_2) expressed osteocalcin, dentin matrix protein 1 (DMP1), and matrix extracellular phosphoglycoprotein (MEPE) (mature osteoblast/osteocyte markers), whereas expression of alpha smooth muscle actin (SMA) and calponin [markers of smooth muscle cells (SMCs)] was down regulated after 4 weeks (Figure 2). Conversely, cells cultured under hypoxic conditions (5% O_2) still expressed smooth muscle markers after 4 weeks and showed lower expression of osteoblast/osteocyte markers (Figure 2). Alkaline phosphatase (ALP) activity and mineralization (von Kossa stain) were also reduced by hypoxic culture (Figure 3). These in vitro observations demonstrate that VSMCs differentiate into osteogenic cells when exposed to a relatively high oxygen tension (normoxia), whereas hypoxia maintains the SMC phenotype. The regulation of VSMC differentiation by oxygen tension demonstrated in this study may be of a fundamental importance for various pathophysiologic processes involving these cells.

Naomi Yamasaki and Makoto Hirao contributed equally to this work.

Correspondence to: Makoto Hirao